Wiley
Journal of Mathematics
Volume 2024, Article ID 5329529, 25 pages
https://doi.org/10.1155/jom/5329529

WILEY

Research Article

A New Heavy-Tailed Lomax Model With Characterizations, Applications, Peaks Over Random Threshold Value-at-Risk, and the Mean-of-Order-P Analysis

M. I. Khan,[1] Abdussalam Aljadani,[2] Mahmoud M. Mansour ,[3,4] Enayat M. Abd Elrazik,[3,4] G. G. Hamedani,[5] Haitham M. Yousof ,[4] and Wahid A. M. Shehata[6]

[1]*Department of Mathematics, Faculty of Science, Islamic University of Madinah, Madinah 42351, Saudi Arabia*
[2]*Department of Management, College of Business Administration in Yanbu, Taibah University, Al-Munawarah, Al-Madinah 41411, Saudi Arabia*
[3]*Management Information Systems Department, Taibah University, Yanbu 46421, Saudi Arabia*
[4]*Department of Statistics, Mathematics and Insurance, Benha University, Benha, Egypt*
[5]*Department of Mathematical and Statistical Sciences, Marquette University, 1313 W. Wisconsin Ave., Milwaukee, Wisconsin 53233, USA*
[6]*Department of Mathematics, Statistics and Insurance, Faculty of Business, Ain Shams University, Cairo, Egypt*

Correspondence should be addressed to Haitham M. Yousof; haitham.yousof@fcom.bu.edu.eg

Received 29 December 2023; Revised 4 November 2024; Accepted 6 November 2024

Academic Editor: Luigi Rarità

In this work, a new heavy-tailed Lomax model is proposed for the reliability and actuarial risk analysis. Simulations are conducted to investigate how the estimators behave. Parameters are derived through maximum likelihood estimation techniques. The efficacy of the newly proposed heavy-tailed Loma distribution is illustrated using the USA indemnity loss datasets. The findings clearly indicate that the new loss model offers a superior parametric fit compared to other competing distributions. Analyzing metrics such as value-at-risk, tail mean variance, tail variance, peaks over a random threshold value-at-risk (PORT-VAR), and the mean-of-order-P ($\mathrm{MOP}_{(P)}$) can aid in risk assessment and in identifying and describing significant events or outliers within the USA indemnity loss. This research introduces PORT-VAR estimators tailored specifically for risk analysis using the USA indemnity loss dataset. The study emphasizes determining the optimal order of P based on the true mean value to enhance the characterization of critical events in the dataset.

Keywords: characterizations; insurance data; Lomax model; mean-of-order-P; peaks over random threshold; statistical molding; times of failure; times of service; USA indemnity loss; value-at-risk

1. Introduction

In economics, insurance, business, risk analysis, and actuarial science, the Lomax (LO) distribution (see LO [1]), also known as the Type II Pareto model, is widely utilized. Statisticians and economists have long been fascinated by its heavy-tailed properties and its application in various mathematical and statistical modeling techniques. The LO distribution (see Tadikamalla [2]; Cordeiro, Ortega, and Popović [3]; Aboraya [4]; Refaie [5]; and Corbellini et al. [6]) has proven invaluable in practical fields such as reliability, insurance, engineering, and actuarial sciences. Over time, researchers have extended its applications in diverse directions, each extension offering unique utility and characteristics. Recently, the LO distribution has found new applications in testing statistical hypotheses using both censored and uncensored samples.

The LO distribution is employed to model extreme events or tail risks in insurance claims' data. It provides a flexible framework for capturing high-frequency, lowprobability events that are crucial for assessing risk. Insurance companies use the LO distribution to model the distribution of potential losses, which helps in determining adequate reserves and pricing premiums. Actuaries utilize the LO distribution to analyze and forecast future claims and liabilities. Its ability to handle heavy-tailed data makes it suitable for assessing the financial health and stability of insurance portfolios. Moreover, in reinsurance, where insurers transfer portions of their risk to other parties, the LO distribution aids in understanding the distribution of risks across different layers of coverage (see Xie and Lai [7]; Asimit and Jones [8]; Klugman, Panjer, and Willmot [9]; Tang and Wang [10]; and McNeil, Frey, and Embrechts [11]). The continuous LO distribution's survival function (RF) or reliability is supplied as

$$R_{\xi}(y)\big|(y\geq 0,\xi>0)=(1+0.5y)^{-\xi}, \tag{1}$$

where the positive parameter ξ of the continuous LO distribution

$$H_{\xi}(y)=1-R_{\xi}(y)\big|(y\geq 0,\xi>0), \tag{2}$$

is the LO cumulative distribution function (CDF). In this study and depending on the LO model, we propose a novel heavy-tailed LO model called generalized exponential LO (GELO) designed for reliability and actuarial risk analysis. Our approach involves conducting simulations to assess the behavior of estimators. Parameters are estimated using maximum likelihood estimation techniques to ensure robustness and accuracy. To demonstrate the effectiveness of our newly proposed heavy-tailed LO distribution, we utilize datasets from USA indemnity losses. Our findings unequivocally show that our model outperforms other existing distributions in terms of parametric fit. We employ various metrics, including value-at-risk (VAR), tail mean variance (T-MV), tail VAR (T-VAR), tail variance (TV), peaks over a random threshold VAR (PORT-VAR), and the mean-of-order-P ($\mathrm{MOP}_{(P)}$), to facilitate risk assessment (see McNeil, Frey, and Embrechts [11]; Klugman, Panjer, and Willmot [9]; and Mohamed et al. [12]). These metrics not only aid in quantifying risks but also assist in identifying and characterizing significant events or outliers within the USA indemnity loss dataset. A key contribution of this research is the development of PORT-VAR estimators tailored specifically for analyzing risks inherent in the USA indemnity loss dataset. Emphasis is placed on determining the optimal order of P ($\mathrm{OO}_{(P)}$) based on the true mean value (TMV), thereby enhancing our ability to discern critical events and their implications within the dataset. This approach enhances our understanding of risk dynamics and supports informed decision-making in the insurance and financial sectors. The new model was also applied to data related to reliability in order to demonstrate the flexibility and importance of the new distribution. However, the insurance case study is the most recent contribution of this paper. As per Alizadeh et al. [13], the CDF of GELO model is given as

$$F\left(y\mid \underline{\varsigma}\right)=\left(1-\exp\left(-\left\{[-\mathfrak{z}(y)+1]^{a_2}-1\right\}^{-1}\right)\right)^{a_1}\Big|\left(\underline{\varsigma}=a_1,\xi,a_2\right), \tag{3}$$

where $\mathfrak{z}(y)=(1+0.5y)^{-\xi}$. The probability density function (PDF) corresponding to (3) can be obtained as

$$f\left(y\mid \underline{\varsigma}\right)=a_1(\xi/2)a_2\frac{[-\mathfrak{z}(y)+1]^{a_2-1}(1+0.5y)^{-(\xi+1)}A_{a_2,a_1,\xi}(y)}{\exp\left(\left\{[-\mathfrak{z}(y)+1]^{-a_2}-1\right\}^{-1}\right)\left\{1-[-\mathfrak{z}(y)+1]^{a_2}\right\}^{2}}, \tag{4}$$

where $a_1,a_2>0$ are two additional parameters which control the shape of the density, and

$$A_{a_2,a_1,\xi}(y)=\left[1-\exp\left(-\left\{[-\mathfrak{z}(y)+1]^{-a_2}-1\right\}^{-1}\right)\right]^{a_1-1}. \tag{5}$$

The hazard/failure rate function (HzRF) of our RV Y can be derived from $h_{\underline{\varsigma}}(y)=f(y\mid\underline{\varsigma})/[1-F(y\mid\underline{\varsigma})]$. If $\sim u(0,1)$, then

$$y_u=2\left[\left(1-\left\{-\log\frac{[w(u,a_1)]}{[1-\log(w(u,a_1))]}\right\}^{1/a_2}\right)^{-(1/\xi)}-1\right], \tag{6}$$

has CDF in (3) where $w(u,a_1)=1-u^{1/a_2}$. This formula is used in simulations and mathematical modeling when necessary to evaluate different estimation methods. For investigating the adaptability, importance and flexibility of the novel density, as well as the HzRF that corresponds to it, we present Figure 1 (the panel on the left is for the new density, and the panel on the right is for the HzRF that corresponds to it). Based on the left plot in Figure 1, it has been observed that the novel PDF can be "asymmetric," "right-skewed PDF" with significant tail or "right-skewed PDF" with only one peak and light tail. The new LO probability distribution can have flattened peaks and sharp, pointed peaks. According to Figure 1 (the right plot), it is possible for the HzRF of the GELO model to exhibit the following behaviors: "decreasing then constant HzRF," "monotonically increasing HzRF," "U-HzRF," and "constant HzRF."

Recent advancements in statistical modeling and its applications in risk management and actuarial sciences have been substantial, driven by the increasing demand for sophisticated frameworks that can handle diverse datasets and complex risk scenarios. Hamed, Cordeiro, and Yousof [14] introduce a compound LO model designed for negatively skewed insurance claims' data, focusing on copula-based modeling and risk assessment. Yousof et al. [15] and Yousof et al. [16] offer a new reciprocal Weibull extension aimed at extreme value modeling and risk assessment in insurance. Ibrahim et al. [17] explore both Bayesian and non-Bayesian methods for analyzing risk in left-skewed insurance data. Yousof et al. [18] further advanced risk analysis by examining bimodal heavy-tailed Burr XII models in insurance contexts. These contributions highlight the ongoing development and application of advanced statistical models in tackling complex risk management issues across various fields (for more applications, see Elbatal et al. [19]; Hashempour, Alizadeh, and Yousof [20]; Alizadeh et al. [21]; Salem et al. [22]; Hamedani et al. [23]; and Alizadeh et al. [24]). For more details and applications, see Marshall and Siegel [25]; Best [26]; Syuhada, Tjahjono, and Hakim [27]; Cordero-Romero and Benito-Muela [28]; Benito, López-Martín, and Navarroet al. [29]; Refaie and Ali [30]; Refaie et al. [31]; and Martín [32].

These insights provide a comprehensive view of the distribution's properties and its implications across different scenarios. Generally, we are motivated to present this work for the following reasons:

- The paper introduces a new heavy-tailed LO model specifically tailored for reliability and actuarial risk analysis. This model represents an advancement in statistical techniques applied to insurance and financial risk management.
- Introducing several novel, unique models with various hazard rate functions including "increasing HzRF" "decreasing then constant HzRF," "monotonically growing HzRF," "bathtub HzRF (U-HzRF)," and "constant HzRF." The distribution's elasticity increases as the variety of failure rate types increases. The adoption of these forms will make the work of a great number of statisticians as well as practitioners easy who might employ the new distribution in the modeling of real-life data. Validating the failure rate function for this aim was an issue that received a lot of attention and consideration from us (see Figure 1).
- The reliability datasets involve a bimodal density form and a semisymmetric kernel density estimation (KDE) that is somewhat tilted to the left (see Figure 2).
- The environmental real datasets that are not symmetric but do not have any observations that are excessive, as shown in Figures 3 and 4.
- The environmental and real-life datasets which have increasing HzRF are illustrated in Figure 5.
- The GELO model is analyzed and then compared with many other relevant and nested models in analyzing and modeling the reliability and times of failure of the airplane windscreen datasets.
- By employing a range of metrics such as VAR, T-MV, TV, and PORT-VAR, the study provides comprehensive tools for assessing and quantifying risks. These metrics enable a deeper understanding of risk dynamics and facilitate proactive risk management strategies.
- This work identifies and characterizes significant events and outliers within the USA indemnity loss dataset. This capability is crucial for insurers and risk managers seeking to mitigate unexpected losses and optimize their risk portfolios.
- The study emphasizes the importance of determining the ($OO_{(P)}$) based on TMVs. This approach enhances the precision of risk characterization and decision-making processes, contributing to more effective risk management strategies.
- Introducing PORT-VAR estimators tailored for the USA indemnity loss dataset, which addresses a specific need in risk analysis. This customization enhances the relevance and applicability of the research findings in practical insurance and financial contexts.
- The use of simulations and maximum likelihood estimation techniques to derive model parameters ensures rigorous statistical foundations. This methodological rigor enhances confidence in the model's accuracy and applicability in real-life scenarios.

2. Characterizations and Some Properties

2.1. Characterization in Terms of the RvHF. The RvHF, $r_F(y \mid \underline{\varsigma})$, of a certain CDF, F, which is a twice differentiable is presented as

$$r_F\left(y \mid \underline{\varsigma}\right) = \frac{f\left(y \mid \underline{\varsigma}\right)}{F\left(y \mid \underline{\varsigma}\right)}. \tag{7}$$

Proposition 1. *Let $Y|Y\colon \mathfrak{Z} \longrightarrow (0,\infty)$ be a certain C-RV. The PDF of RV is Y if and only if the following differential equation holds*

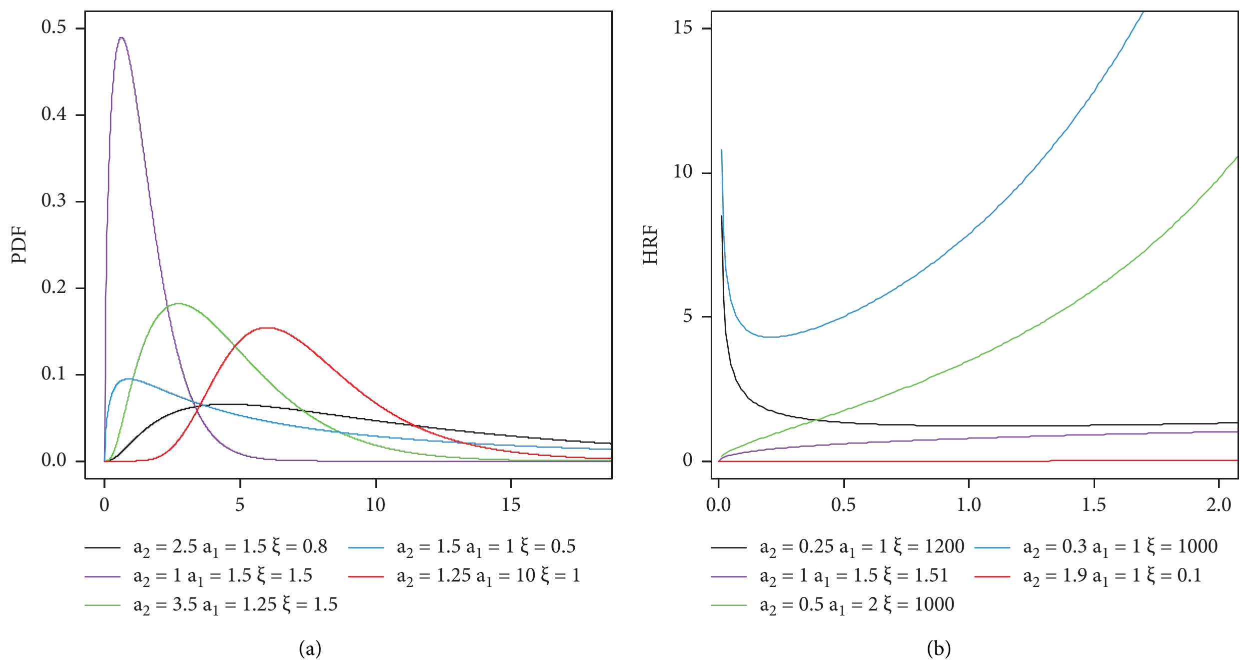

Figure 1: PDF shapes (a) and its relevant HRF shapes (b) under some parameters value.

$$r_F'\left(y \mid \underset{\smile}{\varsigma}\right) + \frac{1}{2}(1+0.5y)^{-1} r_F(y)(1+\zeta) = a_1 a_2 \left(\frac{\zeta}{2}\right)(1+0.5y)^{-(1+\zeta)} \frac{d}{dx}\mathfrak{z}(y;\xi,a_2), \quad y>0, \tag{8}$$

where

$$\mathfrak{z}(y;\xi,a_2) = \frac{[-\mathfrak{z}(y)+1]^{a_2-1}}{\left\{1-[-\mathfrak{z}(y)+1]^{a_2}\right\}^2 \exp\left(-\left\{[-\mathfrak{z}(y)+1]^{a_2}-1\right\}^{-1}\right)}. \tag{9}$$

The proof is simple and left out as a result.

2.2. Characterization Based on the CEx. This approach is often used in statistics and probability theory to gain insights into the properties of a RV or distribution.

Proposition 2. *Let $Y|Y\colon \mathfrak{z} \longrightarrow (0,\infty)$ be a C-RV with a certain CDF $(y \mid \underset{\smile}{\varsigma})$. Let $V(y)$ be a differentiable function on (e,f) with $\lim_{y\longrightarrow f} V(y \mid \underset{\smile}{\varsigma}) = 1$. Then, for $\delta \neq 1$,*

$$\frac{1}{\delta}E\left[V\left(y \mid \underset{\smile}{\varsigma}\right) \mid Y \le y; y \in (e,f)\right] = \psi\left(y \mid \underset{\smile}{\varsigma}\right), \tag{10}$$

implies that

$$V\left(y \mid \underset{\smile}{\varsigma}\right)|Y \le y; y \in (e,f) = \left[F\left(y \mid \underset{\smile}{\varsigma}\right)\right]^{(1/\delta)-1}. \tag{11}$$

Remark 1. For

$$V\left(y \mid \underset{\smile}{\varsigma}\right) = 1 - \exp\left(-\left\{[-\mathfrak{z}(y)+1]^{a_2}-1\right\}^{-1}\right), \quad \delta = a_1\frac{1}{a_1+1}. \tag{12}$$

A description of the GELO distribution is supplied by Proposition 1. See Glänzel [33]; Papathanasiou [34]; and Glänzel [35] and Hosking [36] for more results.

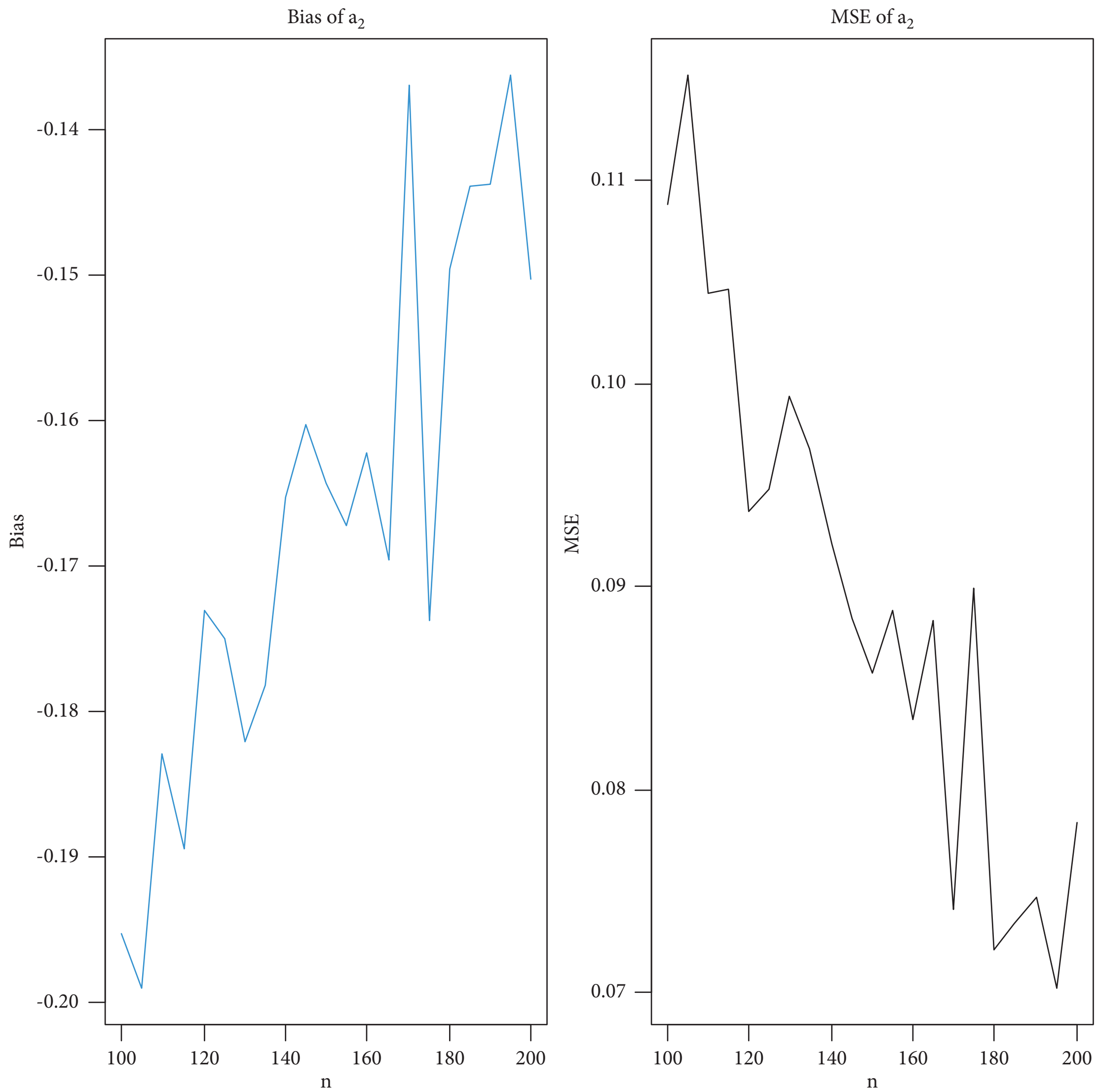

FIGURE 2: The parameter a_2's biases and MSEs.

3. Properties

3.1. Moments and Moment Generating Function (MOGF). Consider the following exponential series:

$$\left(\frac{1-\varsigma_1}{\varsigma_2}\right)^{\varsigma_3-1} = \sum_{\varsigma_4=0}^{\infty} (-1)^{\varsigma_4} \left(-\varsigma_1\right)^{\varsigma_4} \binom{\varsigma_3-1}{\upsilon} \left(\frac{1}{\varsigma_2}\right)^{\varsigma_4} \left\|\frac{\varsigma_1}{\varsigma_2}\right| < 1, \quad \varsigma_3 > 0, \tag{13}$$

where ς_3 is a real and noninteger. Then, expanding the quantity $A_{a_2,a_1,\xi}(y)$ by using $(1-\varsigma_1/\varsigma_2)^{\varsigma_3-1}$, we get

$$A_{a_2,a_1,\xi}(y) = \sum_{\upsilon=0}^{\infty} \binom{a_1-1}{\upsilon} (-1)^{\upsilon} \exp\left(-\upsilon\left\{-1+\left[-\mathfrak{z}(0.5y \mid \xi)+1\right]^{-a_2}\right\}^{-1}\right). \tag{14}$$

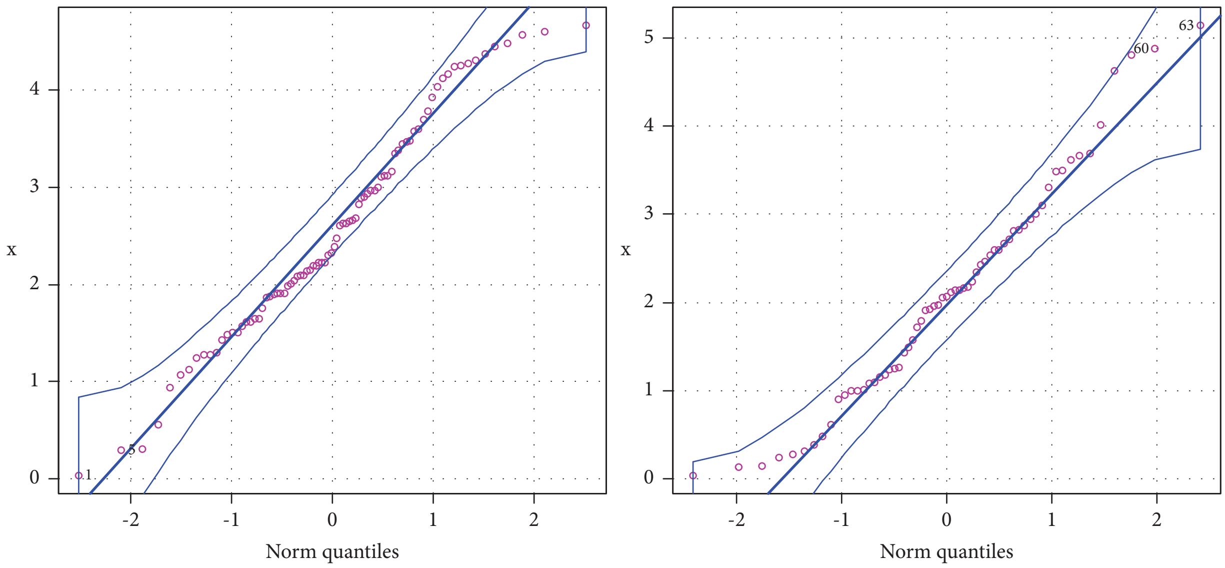

Figure 3: QQ plots.

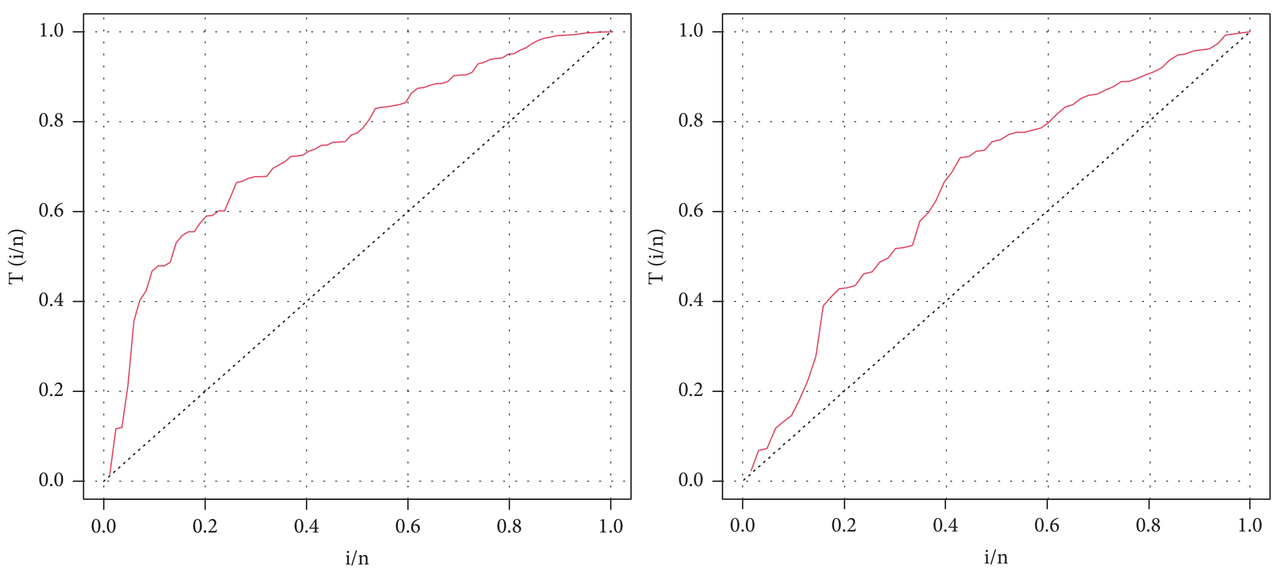

Figure 4: TTT plots.

In light of this, our new PDF of the GELO can be stated as follows:

$$f\left(y \mid \varsigma\right) = \frac{a_1 a_2 (\xi/2)\left[-\mathfrak{z}(0.5y \mid \xi) + 1\right]^{a_2 - 1}}{\left\{1 - \left[-\mathfrak{z}(0.5y \mid \xi) + 1\right]^{a_2}\right\}^2} \sum_{v=0}^{\infty} (-1)^v \binom{a_1 - 1}{v} (1 + 0.5y)^{-(\xi+1)} B_\xi(y), \tag{15}$$

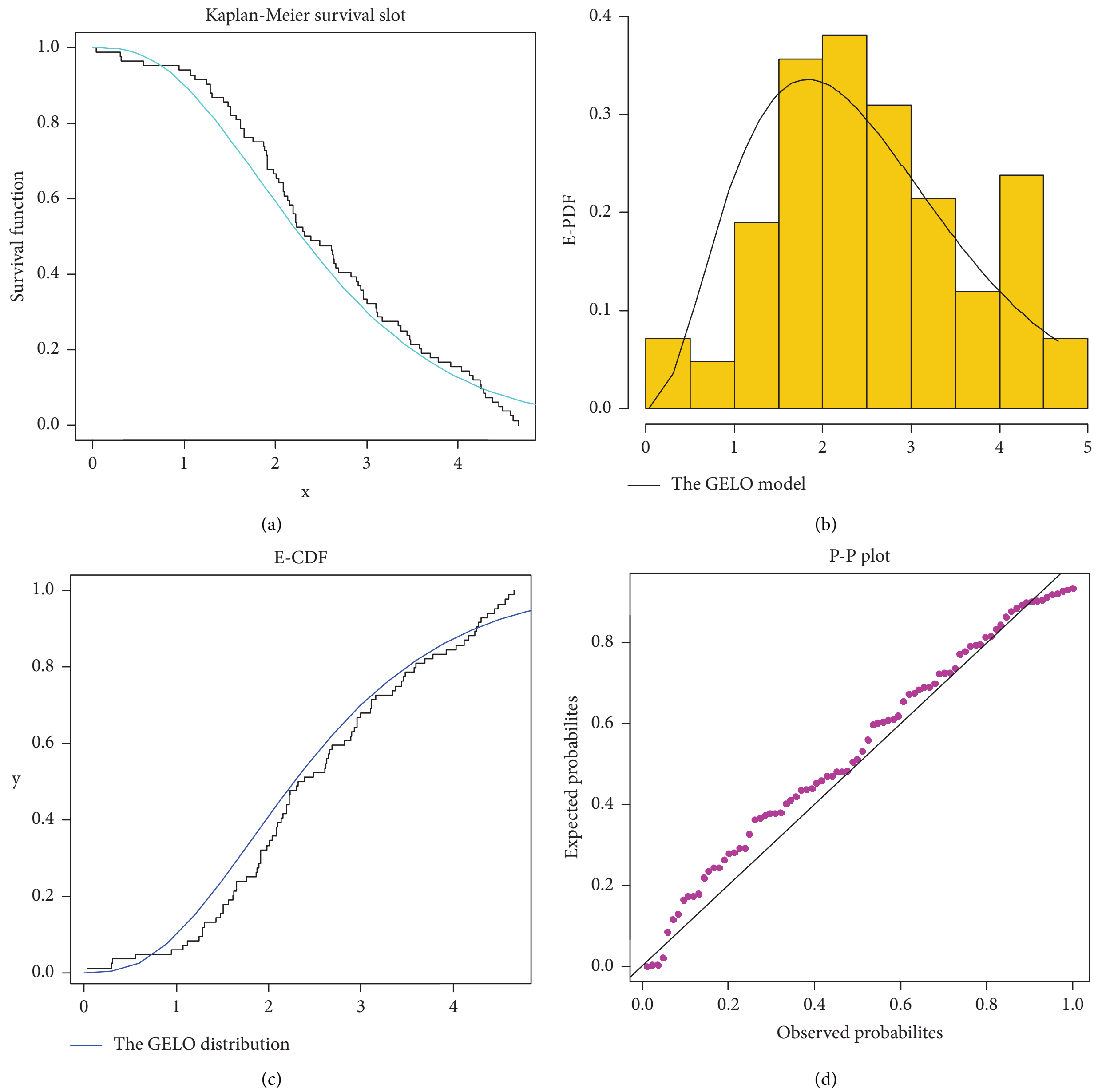

Figure 5: E-KMSF plot (a), E-PDF (b), E-CDF (c), and P–P (d) for Dataset **I**.

where

$$B_{\xi}(y) = \exp\left(-\left\{\left[-\mathfrak{z}(0.5y \mid \xi) + 1\right]^{-a_2} - 1\right\}^{-1}(1+v)\right). \tag{16}$$

Expanding the quantity $B_{\xi}(y)$ by using the power series, we get

$$B_{\xi}(y) = \sum_{k_1=0}^{\infty} \frac{(-1)^{k_1}(1+v)^{k_1}}{k_1!}\left(\frac{\left[-\mathfrak{z}(0.5y \mid \xi) + 1\right]^{a_2 k_1}}{\left\{1 - \left[-\mathfrak{z}(0.5y \mid \xi) + 1\right]^{a_2}\right\}^{k_1}}\right). \tag{17}$$

Then, the PDF in (4) can be formulated as

$$f\left(y \mid \underset{\sim}{\varsigma}\right) = a_1 a_2 (\xi/2) \sum_{k_1,k_2=0}^{\infty} \frac{(-1)^{v+k_1}(1+v)^{k_1}\left[-\mathfrak{z}(0.5y \mid \xi) + 1\right]^{a_2(k_1+1)-1}}{k_1!\underbrace{\left\{1 - \left[-\mathfrak{z}(0.5y \mid \xi) + 1\right]^{a_2}\right\}^{2+k_1}}_{B_{2+k_1,\xi}(y)}} \binom{a_1 - 1}{v} (1+0.5y)^{-(\xi+1)}. \tag{18}$$

Again, applying the series expansion to the quantity $B_{2+k_1,\xi}(y)$, we can get

$$f\left(y \mid \underset{\sim}{\varsigma}\right) = \sum_{k_1,k_2=0}^{\infty} \mathfrak{z}_{k_1,k_2}\, g_{a^{\cdot},\xi}(y)\Big|_{a^{\cdot}=a_2(k_1+k_2+1)}, \tag{19}$$

where

$$g_{a^{\cdot},\xi}(y) = \frac{1}{2} a^{\cdot} \xi \left[1 - (1+0.5y)^{-\xi}\right]^{a^{\cdot}-1} (1+0.5y)^{-(\xi+1)}, \tag{20}$$

represents the exp-LO PDF and then

$$\mathfrak{z}_{k_1,k_2} = \frac{a_1 a_2}{k_1! a^{\cdot}} (-1)^{k_1+k_2} \binom{-(k_1+2)}{k_2} \sum_{v=0}^{\infty} \binom{a_1-1}{v} (v+1)^{k_1} (-1)^{v}. \tag{21}$$

A combination of exp-LO CDFs can also be used to express the corresponding CDF of the GELO probability model. We obtain the same mixture representation by integrating (4) as shown in the following equation:

$$F\left(y \mid \underset{\sim}{\varsigma}\right) = \sum_{k_1,k_2=0}^{\infty} \mathfrak{z}_{k_1,k_2} G_{a^{\cdot},\xi}(y), \tag{22}$$

where $G_{a^{\cdot},\xi}(y) = [1 - (1+0.5y)^{-\xi}]^{a^{\cdot}}$ is the exp-LO CDF. Then, by using (19) and the exp-LO model, the p^{th} ordinary moment of Y can be derived as

$$\Upsilon'_{p,y} = \sum_{k_1,k_2=0}^{\infty} \sum_{\ell=0}^{p} \nabla_{k_1,k_2,\ell}^{(p,a^{\cdot})} B\left(a^{\cdot}, 1 + \frac{\ell - p}{\xi}\right)\Big|_{(\xi>p)}, \tag{23}$$

where

$$\nabla_{k_1,k_2,\ell}^{(p,a^{\cdot})} = \mathfrak{z}_{k_1,k_2} a^{\cdot} 2^{p} (-1)^{\ell} \binom{p}{\ell}, \tag{24}$$

and

$$B(1+\nabla_1, 1+\nabla_2) = \int_0^1 (1-y)^{\nabla_2} y^{\nabla_1} dx. \tag{25}$$

The formula of the MOGF will be obtained from (19) as follows:

$$M_Y(t) = \sum_{k_1,k_2=0}^{\infty} \sum_{\ell=0}^{p} \sum_{p=0}^{\infty} \nabla_{k_1,k_2,\ell,p}^{(p,a^{\cdot})} B\left(a^{\cdot}, 1 + \frac{\ell - p}{\xi}\right)\Big|_{(\xi>p)}, \tag{26}$$

where

$$\nabla_{k_1,k_2,\ell,p}^{(p,a^{\cdot})} = \frac{1}{p!} t^{p} \nabla_{k_1,k_2,\ell}^{(p,a^{\cdot})}. \tag{27}$$

3.2. Reliability Functions and Entropies.

The residual life of Y at the n th instant is supplied by

$$w_{n,Y}(t) = \frac{1}{1 - F_{\underset{\sim}{\varsigma}}(t)} \sum_{k_1,k_2=0}^{\infty} \sum_{p}^{n} \sum_{\ell=0}^{n} L_{k_1,k_2,p,\ell}^{(n,a^{\cdot})} \left[B\left(a^{\cdot}, 1 + \frac{\ell - n}{\xi}\right) - B_t\left(a^{\cdot}, 1 + \frac{\ell - n}{\xi}\right)\right]\Bigg|_{(n=1,2,\ldots,\xi>n)}, \tag{28}$$

where

$$L_{k_1,k_2,p,\ell}^{(n,a^{\cdot})} = \binom{n}{p} (-t)^{n-p} \mathfrak{z}_{k_1,k_2} a^{\cdot} 2^{p} (-1)^{\ell} \binom{p}{\ell}, \tag{29}$$

and

$$B_{\nabla_3}(1+\nabla_1, 1+\nabla_2) = \int_0^{\nabla_3} (1-y)^{\nabla_2} y^{\nabla_1} dx. \tag{30}$$

Conversely, the n th moment of reversed residual life turns into

$$W_{n,Y}(t) = \frac{1}{F_{\underset{\sim}{\varsigma}}(t)} \sum_{k_1,k_2=0}^{\infty} \sum_{p=0}^{n} \sum_{\ell=0}^{n} L_{k_1,k_2,\ell}^{(n,a^{\cdot})} B_t\left(a^{\cdot}, 1 + \frac{\ell - n}{\xi}\right)\Big|_{(n=1,2,\ldots,\xi>n)}, \tag{31}$$

where

$$L^{(n,a^{\cdot})}_{k_1,k_2,p,\ell} = (-1)^p \binom{n}{p} t^{n-p} \mathfrak{z}_{k_1,k_2} a^{\cdot} 2^p (-1)^\ell \binom{p}{\ell}. \tag{32}$$

In this part, we shall analyze some different types of entropies such as the Rényi entropy (RN-E) and the p-entropy ($-E$). The definition of the RN-E is

$$R_\lambda(y) = \frac{1}{1-\lambda} \log \Upsilon^{+\infty}_{-\infty}\left[\lambda; f\left(y \mid \underline{\varsigma}\right)\right]\Big|_{(\lambda>0 \text{ and } \lambda\neq 1)}, \tag{33}$$

where $\Upsilon^{+\infty}_{-\infty}[\lambda; f(y \mid \underline{\varsigma})] = \int_{-\infty}^{\infty} [f(y \mid \underline{\varsigma})]^\lambda dx$. Using the PDF presented in (19), we have

$$\left[f\left(y \mid \underline{\varsigma}\right)\right]^\lambda = \sum_{k_1,k_2=0}^{\infty} (1+0.5y)^{-\lambda(\xi+1)} L^{(\lambda)}_{k_1,k_2} \left[-\mathfrak{z}(0.5y \mid \xi)+1\right]^{a_2(k_1+k_2+\lambda)-\lambda}, \tag{34}$$

where

$$L^{(\lambda)}_{k_1,k_2} = \left(\frac{a_1 a_2 \xi}{2}\right)^\lambda \frac{(-1)^{k_1+k_2}}{k_1!} \sum_{v=0}^{\infty} (v+\lambda)^{k_1} (-1)^v \binom{-(k_1+2)}{k_2} \binom{\lambda(a_1-1)}{v}. \tag{35}$$

Next, the GELO model's RN-E is supplied with

$$R(y \mid \lambda) = \log \frac{\left[\sum_{k_1,k_2=0}^{\infty} v_0^{+\infty}(y;\lambda) L^{(\lambda)}_{k_1,k_2}\right]}{[1-\lambda]}, \tag{36}$$

where

$$v_0^{+\infty}(y;\lambda) = \int_0^{\infty} (1+0.5y)^{-\lambda(\xi+1)} \left[-\mathfrak{z}(0.5y \mid \xi)+1\right]^{a_2(k_1+k_2+\lambda)-\lambda} dx. \tag{37}$$

The $-E$ ($H(y \mid p)$) can then be derived using the following formula:

$$H(y \mid p) = \frac{\log\left\{1 - \left[\sum_{k_1,k_2=0}^{\infty} v_0^{+\infty}(y;p) L^{(p)}_{k_1,k_2}\right]\right\}}{[p-1]}, \tag{38}$$

where

$$L^{(p)}_{k_1,k_2} = \left(\frac{a_1 a_2 \xi}{2}\right)^p \frac{(-1)^{k_1+k_2}}{k_1!} \sum_{v=0}^{\infty} (-1)^v (v+p)^{k_1} \binom{-(k_1+2)}{k_2} \binom{p(a_1-1)}{v}\Bigg|_{(p>0, p\neq 1)}. \tag{39}$$

3.3. Stochastic Properties. Suppose $Y_1 \sim$ GELO ($\underline{\varsigma}_1$) and $Y_2 \sim$ GELO ($\underline{\varsigma}_2$). Then, Y_1 is stochastically smaller than Y_2 if $a_{21} > a_{22}$ and $a_{11} > a_{12}$. Note that, for any $a_1 > a_2$,

$$\log \mathfrak{z}_{\xi_1}(y_1) = -\xi_1 \log\left(\left(\frac{y_1}{2}\right)+1\right), \mathfrak{z}_{\xi_2}(y_2) = -\xi_2 \log\left(\left(\frac{y_2}{2}\right)+1\right), \tag{40}$$

we have $[1-\mathfrak{z}_{\xi_1}(y_1)]^{a_{21}} > [1-\mathfrak{z}_{\xi_2}(y_2)]^{a_{22}}$. Then, we have

$$-\frac{\left[1-\mathfrak{z}_{\xi_1}(y_1)\right]^{a_{21}}}{1-\left[1-\mathfrak{z}_{\xi_1}(y_1)\right]^{a_{21}}} < -\frac{\left[1-\mathfrak{z}_{\xi_2}(y_2)\right]^{a_{22}}}{1-\left[1-\mathfrak{z}_{\xi_2}(y_2)\right]^{a_{22}}}, \tag{41}$$

then

$$\longrightarrow \left(1-\exp\left\{-\frac{\left[1-\mathfrak{z}_{\xi_1}(y_1)\right]^{a_{21}}}{1-\left[1-\mathfrak{z}_{\xi_1}(y_1)\right]^{a_{21}}}\right\}\right)^{a_{11}} > \left(1-\exp\left\{-\frac{\left[1-\mathfrak{z}_{\xi_2}(y_2)\right]^{a_{22}}}{1-\left[1-\mathfrak{z}_{\xi_2}(y_2)\right]^{a_{22}}}\right\}\right)^{a_{12}}, \tag{42}$$

and

$$\longrightarrow 1-\left(1-\exp\left\{-\frac{\left[1-\mathfrak{z}_{\xi_1}(y_1)\right]^{a_{21}}}{1-\left[1-\mathfrak{z}_{\xi_1}(y_1)\right]^{a_{21}}}\right\}\right)^{a_{11}} < 1-\left(1-\exp\left\{-\frac{\left[1-\mathfrak{z}_{\xi_2}(y_2)\right]^{a_{22}}}{1-\left[1-\mathfrak{z}_{\xi_2}(y_2)\right]^{a_{22}}}\right\}\right)^{a_{12}}. \tag{43}$$

This completes the proof. For a portfolio of assets where each asset return follows a GELO distribution, conditions are established under which the overall portfolio return distribution is stochastically smaller than a reference portfolio. If the weights assigned to each asset are adjusted such that the effective parameters (mean, variance, and shape) of the portfolio returns result in a decrease compared to the reference portfolio, then the risk (measured by quantiles or other risk metrics) of the portfolio is lower.

4. Estimation

To ascertain the MAXLE of $\underline{\varsigma}$, the log-likelihood function is derived. Then, it is simple to derive the score vector's components. The MAXLE is obtained by setting the equations of the obtained nonlinear system $U_{a_1}=0, U_{a_2}=0, U_{\xi}=0$ and solving them concurrently. The quasi–Newton algorithms are used to solve the maximum likelihood nonlinear system of equations, keeping in mind that the success of the quasi–Newton algorithm depends on the nature of the likelihood function and the chosen optimization parameters. In some cases, the function may not be well-behaved, and additional precautions or algorithm adjustments may be necessary. The quasi–Newton algorithm iteratively updates the estimate of the parameters related to the novel model based on the observed data and the score function. The general update rule for quasi–Newton methods is to approximate the Hessian matrix (second-order derivative of the log-likelihood) and use it to guide parameter updates. Thus, we initialize an estimate of the Hessian matrix (often known as the identity matrix).

5. Assessing the MAXLE Method

Simulation of a particular distribution of the proposed family is an easy method that can be used to validate the approximation normal distribution for the value of. In this section, a simulation of the GELO model is run. We can conduct the simulation tests to assess the behavior of the finite sample of MAXLEs using the values of biases (Bias) (negative and positive values) and the values of the mean squared errors (MSEs) in a graphic manner. For every n value supplied ($n=50$, 60,200), a replication of $N=1000$ served as the basis for the evaluation. The following main algorithms are considered:

1. Generating $N=1000$ from our GELO model.
2. For a_2, a_1 and ξ and for all samples, compute the MAXLEs.
4. For a_2, a_1 and ξ and for all samples, compute the mean squared errors (*MSEs*) and the Bias given.
5. Repeat these steps for $n|_{(n=n=50,60,\ldots,200)}$, so computing Bias ($\mathrm{Bias}_{\underline{\Theta}}(n)$), the $\mathrm{MSE}_h(n)$ for $h=a_2, a_1$, and ξ and $n|_{(n=50,60,\ldots,200)}$.
6. Figures 2, 6, and 7 give the Bias (the left panels) versus $n=50, 60, \ldots, 200$ and MSEs (the right panels) versus $n=50, 60, \ldots, 200$ for a_2, a_1, and ξ, respectively. The left panels from Figures 2, 6, and 7 show how the Bias vary with respect to the sample size. The right panels from Figures 2, 6, and 7 show how the four MSEs vary with respect to the sample size. From Figures 2, 6, and 7 (the left panels), the Bias for a_2, a_1, and ξ are generally negative and tends to be 0 as $n \longrightarrow \infty$. From Figures 2, 6, and 7 (the right panels), the MSEs decrease to 0 as $n \longrightarrow \infty$.

6. Applications

In this section, we demonstrate the value and adaptability of the GELO model using two applications of real-life data. We contrast the GELO's alignment with a few well-known rival models (see Table 1; for more details about the competitive models, see Tahir et al. [37]; Lemonte and Cordeiro [38];

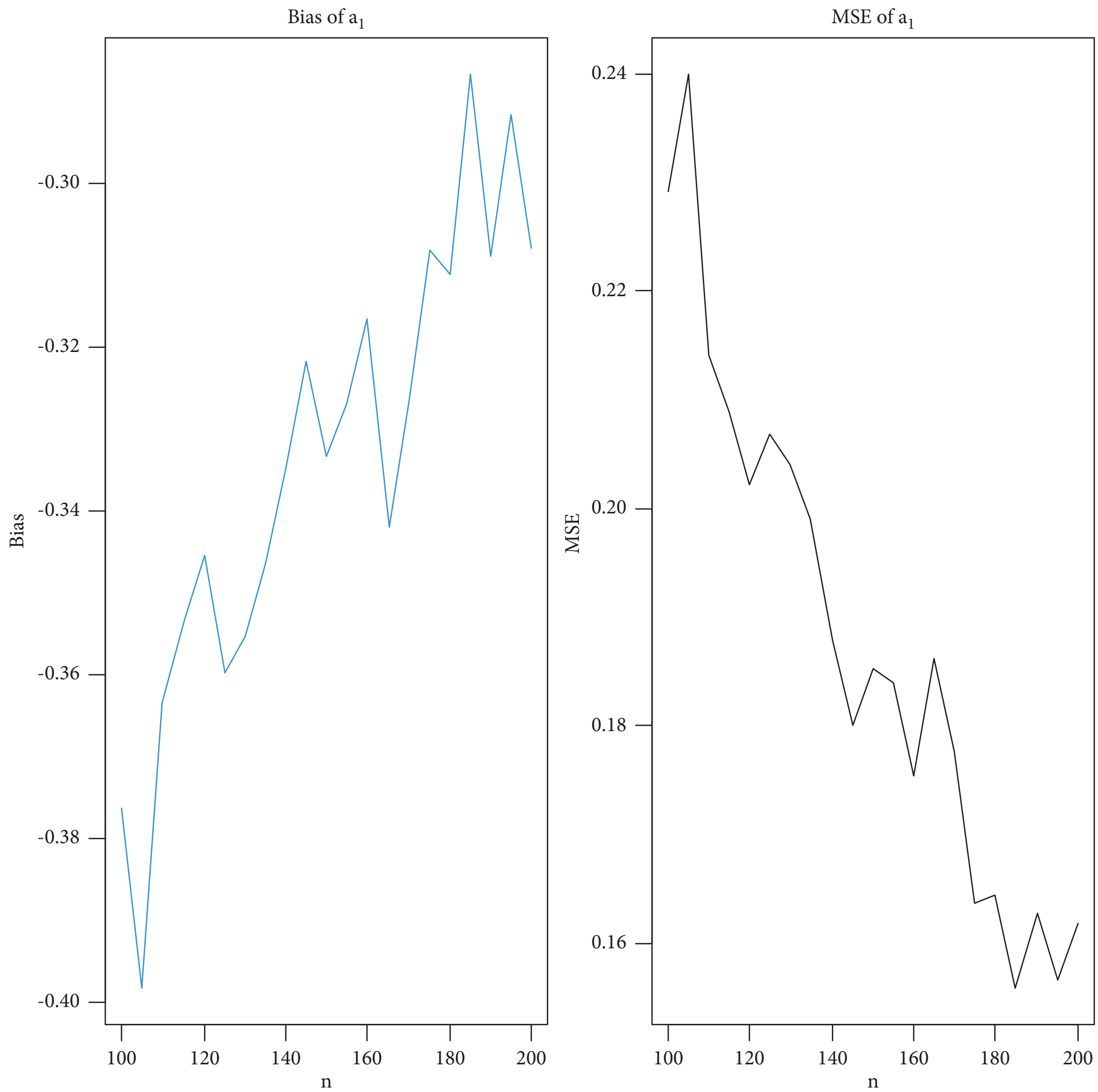

Figure 6: The parameter a_1's biases and MSEs.

Tahir et al. [39]; Khalil and Ali [40]; and Gupta [41]). The data on the "times of failure" of 84 airplane windscreens are provided by Murthy, Xie, and Jiang [42]. The information regarding the "times of service" of 63 airplane windscreens is presented by Murthy, Xie, and Jiang [42]. The non-parametric KDE is offered so that one may study the initial form of real data (for a graphical illustration of this concept, please refer to Figure 8). The box plot that was utilized in the study of the extremes can be found in Figure 9. This plot demonstrates that the investigation did not uncover any extremes, as can be seen from this plot. The quantile–quantile plot, also referred to as the QQ plot (see Figure 3), is sketched out for the purpose of detecting whether the data follow a normal distribution. Simply looking at Figure 4 makes it quite evident that the normality is getting very close to being attained. Investigating the shape of the HzRF can be performed with the use of the total time under test (TTT) plot, which is shown in Figure 5. When we look at Figure 5, we can observe that the HzRF is "increasing HzRF" for both datasets that represent the actual world. Figure 9 displays the estimated Kaplan–Meier survival (E-KMSF) plot, the estimated PDF (E-PDF), the estimated CDF (E-CDF), and the probability–probability (P–P) plot for "times of failure." Figure 10 gives the E-KMSF plot, the E-PDF, the E-CDF, and the P–P plot for "times of failure" and "times of service."

When comparing among some competing models, the following information criteria are utilized: Akaike information criterion (AIC), Anderson–Darling (AD), Bayesian information criterion (BIC), Cramér–von Mises (CvM), consistent AIC (CAIC), and Hannan–Quinn information criterion (HQIC) test . In general, the values of these statistics should be reduced because doing so will result in a better fit for the datasets. The findings of the study of the data pertaining to "times of failure" are shown in Tables 2 and 3, respectively. The MAXLEs as well as the SEs for the "times of failure" data are shown in Table 2. The test statistics for the failure dataset are shown in Table 3. Regarding the

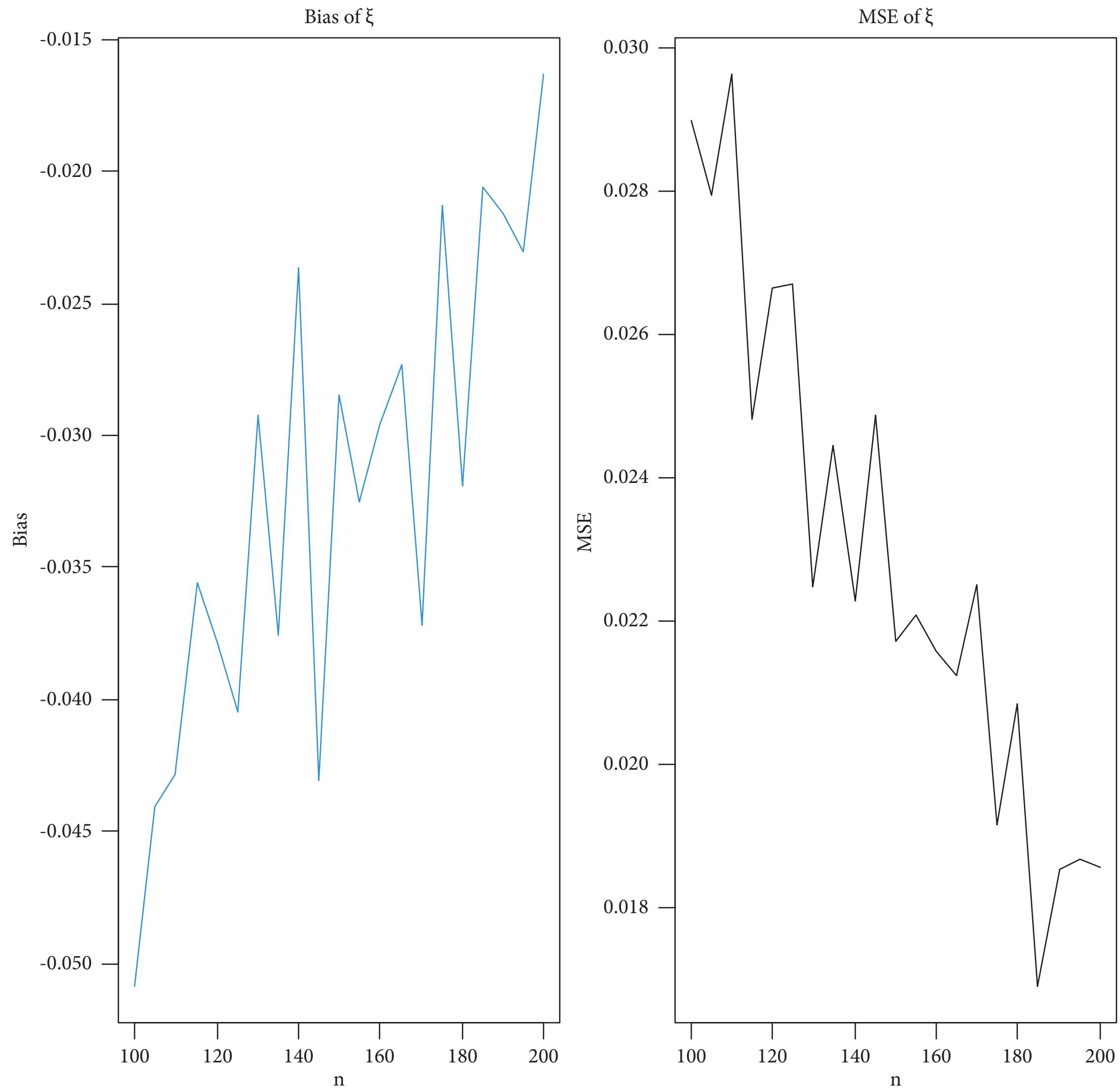

Figure 7: The parameter ξ's biases and MSEs.

Table 1: Competing probability models.

Model (abbreviation)
Lomax (LO), beta LO (BLO), and gamma LO (GLO)
Special generated mixed LO (SGMLO)
Transmuted Topp–Leone LO (TTLO)
Reduced/pseudotransmuted TL LO (RTTLLO)
Odd log-logistic LO (OLLLO), exponentiated LO (exp-LO)
Reduced/pseudo-odd log–logistic LO (ROLLLO)
Reduced/pseudo-Burr–Hatke LO (RBHLO)
Proportional reversed hazard rate Lomax (PRHRLO)

"times of service" data, the findings of the analysis are reported in Tables 4 and 5, respectively. The MAXLEs and SEs for the "times of service" data are presented in Table 4. The test statistics for the service dataset are presented in Table 5. The GELO model offers the lowest values for the AIC, CAIC, BIC, HQIC, AD, and CvM compared to all the fitted models, as seen in Tables 3 and 5. As a result, it is possible to select it as the best model based on these characteristics.

7. Case Study in Insurance With Risk Analysis

In insurance contexts, the PORT-VAR method helps in quantifying the probability and severity of large claims or catastrophic losses, which are crucial for setting adequate reserves and determining reinsurance needs. It provides insights into the average magnitude of losses exceeding a certain threshold, aiding in risk assessment and pricing of insurance products. In this case study, we will employ the new distribution in this context. For this main aim, the VAR, T-MV, tail-VaR (T-VVR), and TV indicators are considered for the GELO distribution under the USA insurance losses.

7.1. MOP$_{(P)}$ Analysis and OO$_{(P)}$. The MOP$_{(P)}$ analysis is a valuable tool in risk analysis for USA indemnity loss data, offering insurers a deeper understanding of the severity and potential frequency of extreme loss events. It supports informed decision-making and strategic planning to effectively manage and mitigate risks in the insurance industry (see

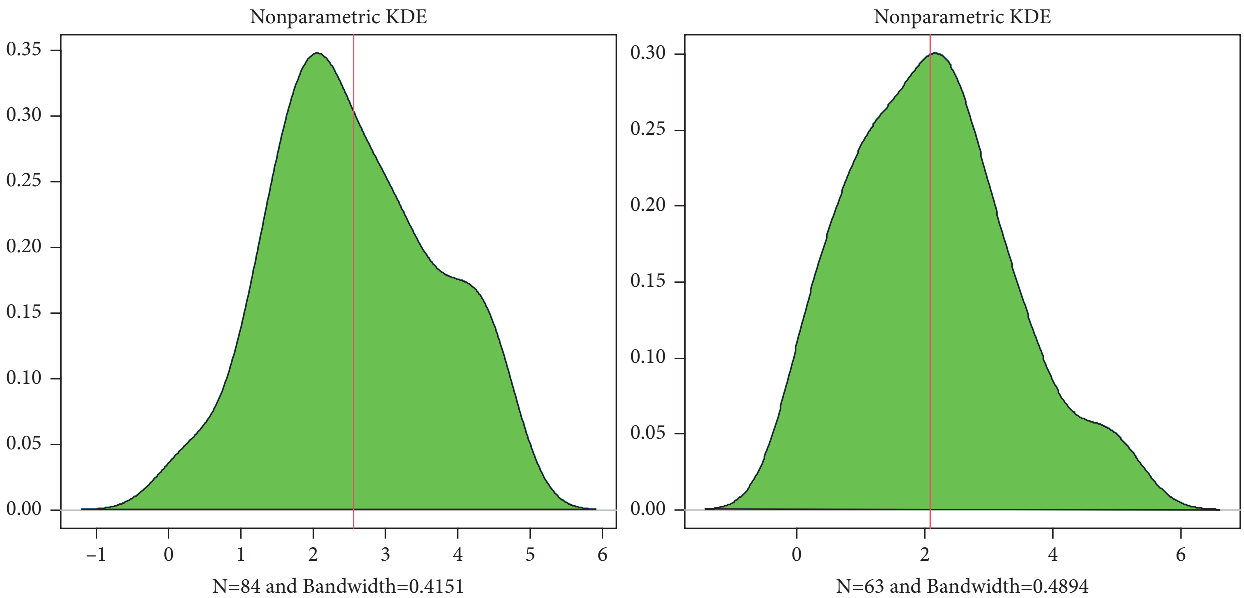

Figure 8: Nonparametric KDE.

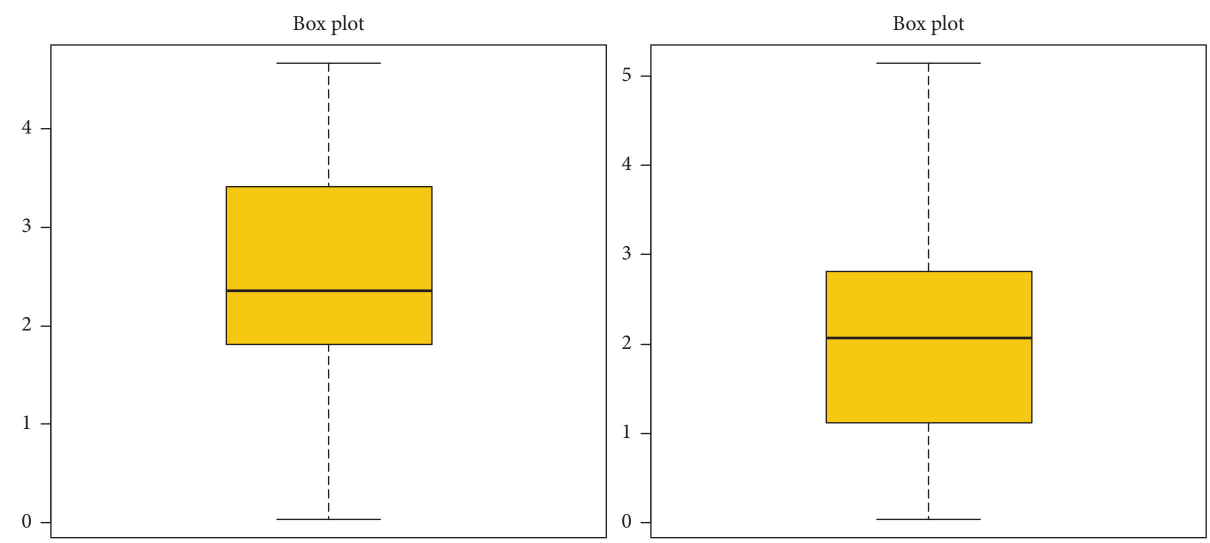

Figure 9: Box plots.

Aljadani [43]). In this subsection, we are interested in $\mathrm{MOP}_{(P)}$ analysis for determining the $\mathrm{OO}_{(P)}$ under the USA indemnity loss data. We consider $P = 1, 2, \ldots, 5$ and $n = 100000$ samples for some initial values of parameters. The TMV, MSE, and Bias are considered in the assessment process.

For all initial values, $P = 5$ shows the lowest MSE and Bias, indicating that it provides the closest approximation to the TMV. As P increases, the $\mathrm{MOP}_{(P)}$ values converge closer to the TMV, reflecting improved accuracy in estimating the true mean. Based on the provided results, $P = 5$ appears to be optimal for this dataset as it minimizes both MSE and bias effectively. This choice suggests that using the top 5 values to estimate the true mean provides the best balance between accuracy and computational efficiency in this scenario. Based on these main important results, we shall consider $P = 5$ in our following risk analysis. Figure 11 gives each indicator v P value. Figure 12 provides the $\mathrm{MOP}_{(P)}$, MSEs, and Bias v P.

7.2. PORT-VAR Estimator for Extreme USA Indemnity Losses. As per Aljadani [43], the PORT-VAR estimator is a specialized tool used by insurers to analyze and quantify tail risks associated with rare yet impactful events in USA indemnity losses. It focuses on extreme events, or "peaks," in claim sizes that surpass a predetermined threshold. This analysis provides insurers with crucial insights into the potential scale of losses beyond conventional risk measures. By identifying and assessing these extreme claims, insurers can better understand vulnerabilities within their portfolios and implement effective risk management strategies. The PORT-VAR analysis, detailed in Table 6 with various confidence levels (CLs) ranging from 50% to 99%,

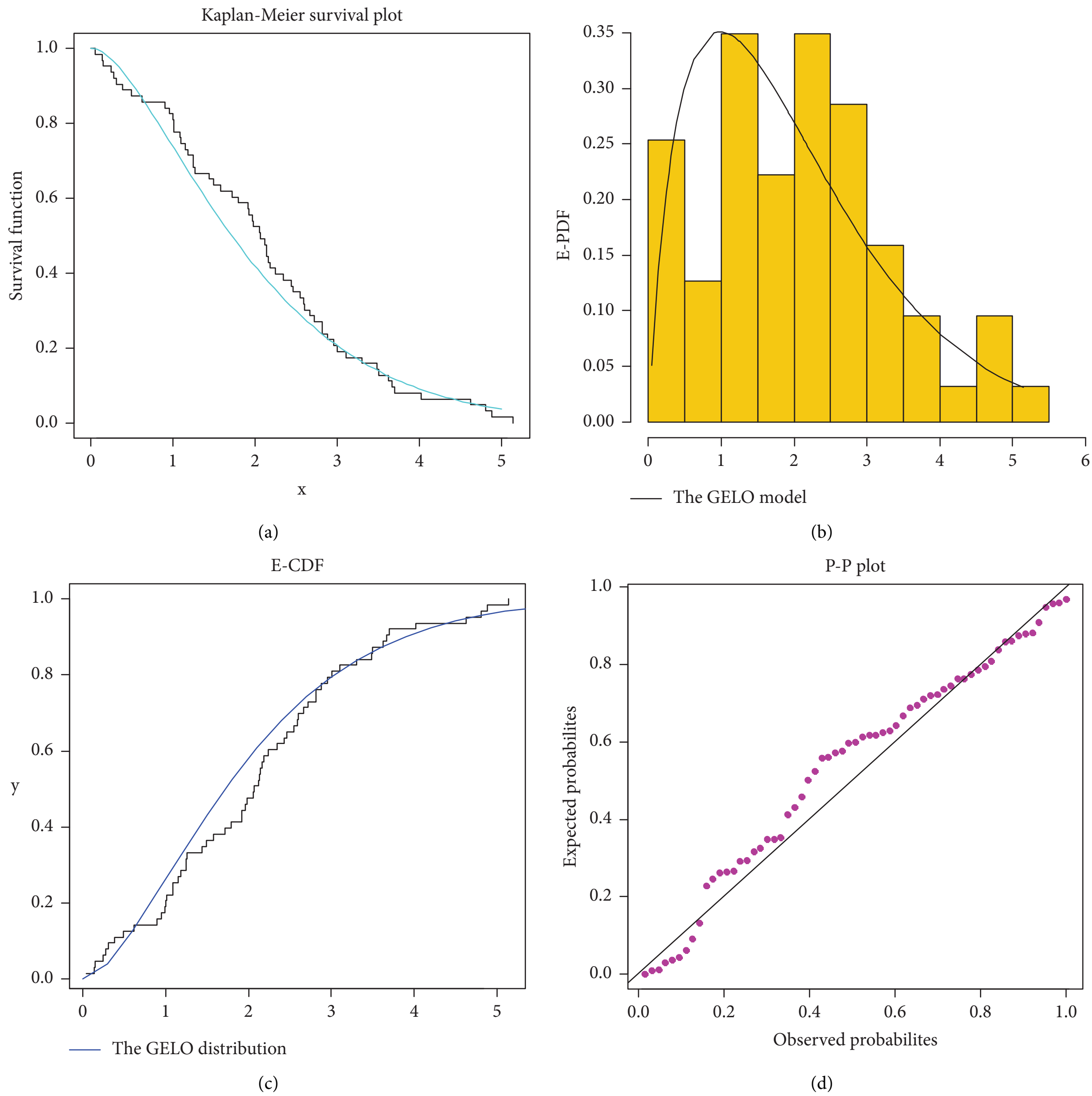

Figure 10: E-KMSF plot (a), E-PDF (b), E-CDF (c), and P–P (d) for Dataset **II**.

illustrates how stricter thresholds at higher CLs lead to the identification of fewer but more significant extreme claims. This relationship informs insurers' risk tolerance assessments and guides their risk management decisions, ultimately enhancing portfolio protection against severe financial impacts. Overall, the PORT-VAR estimator plays a pivotal role in insurers' readiness to handle and mitigate extreme indemnity losses through informed risk management practices.

Table 6 presents a comprehensive analysis using the PORT-VAR method to assess extreme USA indemnity losses across a range of CLs. Each row in the table corresponds to a specific CL, detailing the number of identified extreme loss events (PORT) and key statistical metrics such as minimum, first quartile, median, expected value of extreme losses (ExV), third quartile, and maximum values associated with these events. The number of PORT increases with higher CLs, indicating a stricter criterion for identifying significant deviations in USA indemnity losses. Statistical measures such as minimum, first quartile, median, ExV, third quartile, and maximum values provide insights into the distribution and severity of extreme loss events across different CLs. For example, the maximum values highlight the most severe loss events identified within each CL. This analysis supports

Table 2: Estimates results for "times of failure" data.

Model	Estimates			
GELO (a_2, a_1, ξ)	2.25105 (1.83474)	1.10598 (0.74238)	6254.02 (1836.7)	13,008.3 (573.46)
BLO (a_2, a_1, ξ, σ)	3.60360 (0.6187)	33.63870 (63.7145)	4.83070 (9.2382)	118.837 (428.93)
PRHRLO (a_1, β, ξ)	3.73×10^6 1.01×10^6	4.707×10^{-1} (0.00001)	4.49×10^6 37.14684	
RTTLLO (a_2, a_1, β)	−0.84734 (0.10413)	5.52057 (1.18479)	1.152,144 (0.0959)	
SGMLO (a_1, β, ξ)	-1.04×10^{-1} (0.1223)	9.83×10^6 (4843.3)	1.18×10^7 (501.04)	
GLO (a_1, β, ξ)	3.58760 (0.5133)	52,001.49 (7955.00)	37,029.66 (81.1644)	
Exp-LO (a_1, β, ξ)	3.62610 (0.6236)	20,074.51 (2041.83)	26,257.68 (99.7417)	
ROLLLO (a_2, β)	3.894,502 (0.32221)	0.57316 (0.00922)		
RBHLO (β, ξ)	10,801,754 (983,309)	51,367,189 (232,312)		
LO (β, ξ)	51,425.35 (5933.49) (0.6236)	131,789.8 (296.119) (2041.83)	(99.7417)	
ROLLLO (a_2, β)	3.894,502 (0.32221)	0.57316 (0.00922)		
RBHLO (β, ξ)	10,801,754	51,367,189		

Table 3: Capering model due to "times of failure" data.

Model	$-\ell(\varsigma)$	AIC	CAIC	BIC	HQIC	AD	CvM
GELO	136.2281	278.4562	278.7562	285.7486	281.3877	1.2281	0.14057
GLO	138.4042	282.8083	283.1046	290.1363	285.7559	1.3666	0.1618
BLO	138.7177	285.4354	285.9354	295.2060	289.3654	1.4084	0.1680
Exp-LO	141.3997	288.7994	289.0957	296.1273	291.7469	1.7435	0.2194
ROLLLO	142.8452	289.6904	289.8385	294.5520	291.6447	1.9566	0.2554
SGMLO	143.0874	292.1747	292.4747	299.4672	295.1062	1.3467	0.1578
RTTLLO	153.9809	313.9618	314.2618	321.2542	316.8933	3.7527	0.5592
PRHRLO	162.8770	331.7540	332.0540	339.0464	334.6855	1.3672	0.1609
LO	164.9884	333.9767	334.1230	338.8620	335.9417	1.3976	0.1665
RBHLO	168.6040	341.2081	341.3562	346.0697	343.1624	1.6711	0.2069

comprehensive risk assessment by enabling insurers to gauge the potential impact of extreme loss events and tailor risk management strategies accordingly. Table 6 serves as a valuable tool for insurance professionals, aiding in informed decision-making and proactive risk management in the face of extreme indemnity losses. The detailed statistical breakdown enhances understanding of risk exposures associated with varying confidence thresholds, thereby supporting robust risk assessment and mitigation efforts within the insurance industry.

Based on Table 7, the number of PORTs increases as the CL decreases, indicating a broader coverage of potential extreme events. This approach allows for a comprehensive assessment of the frequency and severity of high-impact events across different risk scenarios. A higher number of PORTs at lower CLs (e.g., 70%–80%) suggests a detailed analysis of more frequent but less severe events. This helps insurers in understanding and managing risks associated with typical occurrences. The concentration of PORTs at higher CLs (e.g., 85%–90%) reflects a focus on extreme and less predictable events, despite their rarity. This strategic allocation of resources ensures readiness for catastrophic events that could significantly impact the insurer. Based on this analysis, we provide some recommendations as follows:

1. Insurance companies should focus on robust risk management strategies that address potential losses at different CLs. This involves understanding the distribution of losses and ensuring adequate capital reserves to cover extreme events.

Table 4: Estimates results for the “times of service” data.

Model	Estimates			
GELO (a_2, a_1, ξ, σ)	2.54613 (0.6276)	0.59372 (0.0947)	110.257 (623.01)	224.619 (450.522)
BLO (a_2, a_1, ξ, σ)	1.92184 (0.3184)	31.2594 (316.841)	4.9684 (50.528)	169.572 (339.21)
TTLO (a_2, a_1, ξ, σ)	(−0.607) (0.21371)	1.785,780 (0.41522)	2123.391 (163.915)	4822.79 (200.01)
PRHRLO (a_1, β, ξ)	1.59×10^6 2.01×10^3	3.93×10^{-1} 0.0004×10^{-1}	1.30×10^6 0.95×10^6	
RTTLLO (a_2, a_1, β)	−0.67145 (0.18746)	2.74496 (0.6696)	1.01238 (0.11405)	
SGMLO (a_1, β, ξ)	-1.04×10^{-1} $(4.1 \times 10^{-1°})$	6.45×10^6 (3.21×10^6)	6.33×10^6 (3.8573)	
OLLLO (a_1, β, ξ)	1.66419 (1.79×10^{-1})	6.34×10^5 (1.7×10^4)	2.01×10^6 7.22×10^6	
GLO (a_1, β, ξ)	1.90733 (0.32133)	35,842.43 (6945.07)	39,197.57 (151.653)	
Exp-LO (a_1, β, ξ)	1.91454 (0.3482)	22,971.15 (3209.53)	32,881.99 (162.230)	
ROLLLO (a_2, β)	2.37233 (0.26825)	0.69109 (0.0449)		
RBHLO (β, ξ)	1,405,552 (422.01)	5,320,342 (28.5232)		
LO (β, ξ)	99,269.8 (11,863.5)	207,019.4 (301.237)		

Table 5: Capering model due to the “times of service” data.

Model	$-\ell(\varsigma)$	AIC	CAIC	BIC	HQIC	AD	CvM
GELO	101.9076	209.8152	210.222	216.2446	212.344	0.9369	0.1553
TTLO	102.4498	212.8996	213.5893	221.4722	216.2713	0.9431	0.1554
GLO	102.8332	211.6663	212.0730	218.0958	214.1951	1.1120	0.1836
SGMLO	102.8940	211.7881	212.1949	218.2175	214.3168	1.1134	0.1839
BLO	102.9611	213.9223	214.6119	222.4948	217.2939	1.1336	0.1872
Exp-LO	103.5498	213.0995	213.5063	219.5289	215.6282	1.2331	0.2037
OLLLO	104.9041	215.8082	216.2150	222.2376	218.3369	0.9424	0.1545
PRHRLO	109.2986	224.5973	225.004	231.0267	227.126	1.1264	0.1861
LO	109.2988	222.5976	222.7976	226.8839	224.2834	1.1265	0.1861
ROLLLO	110.7287	225.4573	225.6573	229.7436	227.1431	2.3472	0.3908

2. The adequacy of capital reserves must be assessed based on the PORT-VAR analysis. It should be ensured that the company’s capital is sufficient to cover losses at higher CLs (e.g., 99% or 95%) to maintain solvency and financial stability.
3. Reinsurance must be considered as a tool to mitigate risk exposure. Reinsurance can help transfer a portion of the risk associated with extreme losses to other insurers or reinsurers, thereby reducing the financial impact on the company.

7.3. VAR Under the USA Indemnity Losses. This section provides a thorough analysis of key risk metrics (VAR, T-VAR, TV, and T-MV) concerning USA indemnity losses, crucial aspects in insurance risk management. These metrics offer vital insights into potential financial exposures linked to indemnity claims. The analysis evaluates these metrics across a spectrum of quantiles, ranging from 70% to 99%. Each quantile represents varying levels of risk, with higher quantiles indicating more severe and less likely scenarios of loss occurrence. By examining these metrics across different quantiles, we gain a nuanced understanding of the distribution and severity of potential indemnity losses under different levels of uncertainty. The assessment of VAR, T-VAR, TV, and T-MV for USA indemnity losses aims to support informed decision-making in risk assessment and mitigation within the insurance industry. By identifying and quantifying potential financial impacts associated with indemnity risks, insurers can strategically allocate resources, establish suitable reserves, and develop robust risk management strategies to safeguard against adverse events. This analysis highlights the importance of employing advanced risk modeling techniques and statistical methodologies to

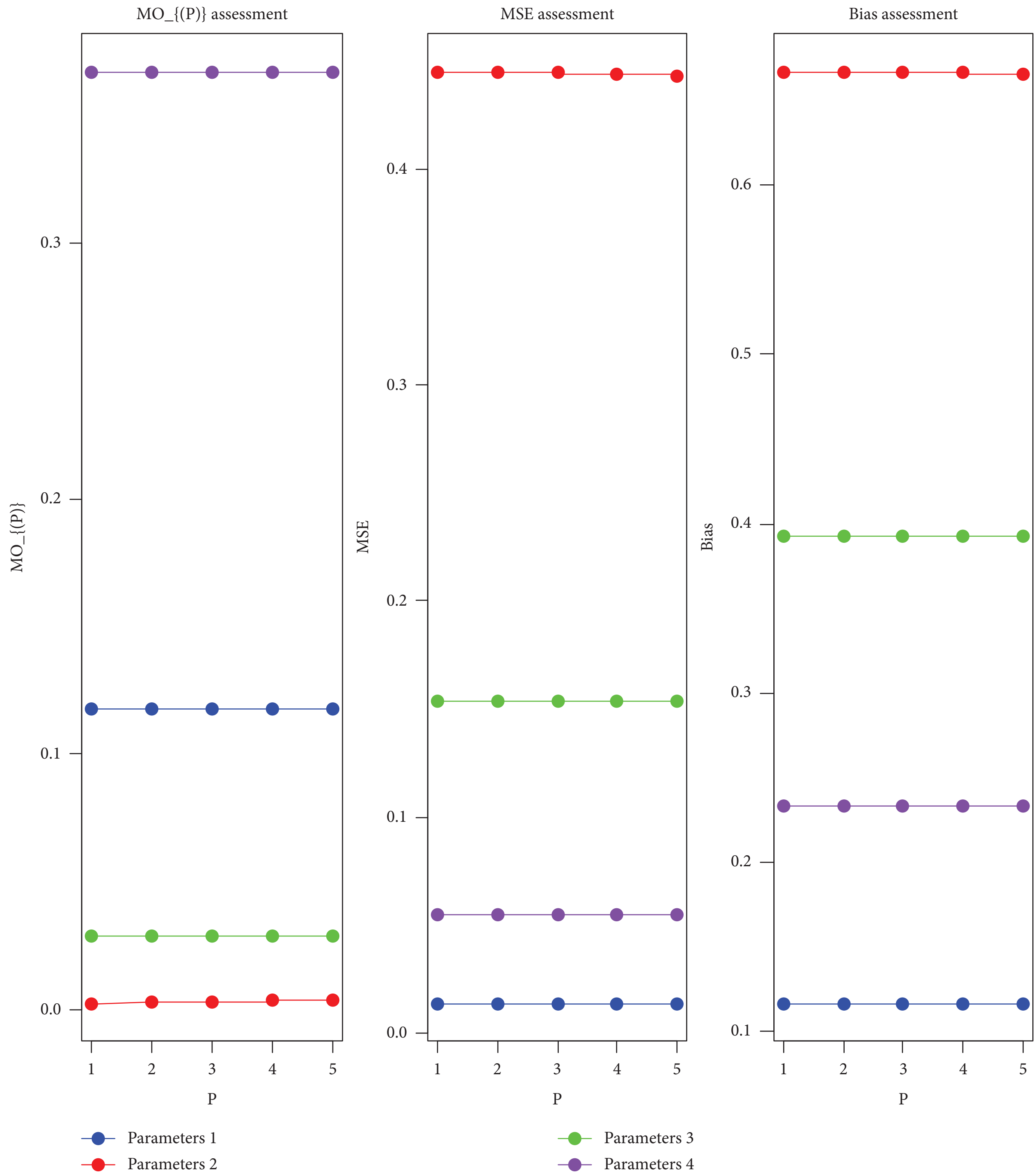

FIGURE 11: Each indicator v P.

effectively manage and mitigate indemnity risks. The insights derived from this analysis play a crucial role in enhancing the resilience and stability of insurance portfolios, contributing significantly to the overall financial health and sustainability of insurance operations amidst evolving risk environments.

Table 8 provides a concise overview of critical risk metrics (VAR, T-VAR, TV, and T-MV) relevant to USA indemnity losses, computed across various quantiles (q) ranging from 70% to 99%. Each quantile signifies a different potential loss level, with higher quantiles indicating more severe scenarios. These metrics are essential for evaluating and mitigating potential indemnity losses, offering insights into the distribution and severity of risks associated with USA indemnity exposures. The values in the Table 8 capture the financial impact corresponding to different probability levels, aiding informed decision-making and risk

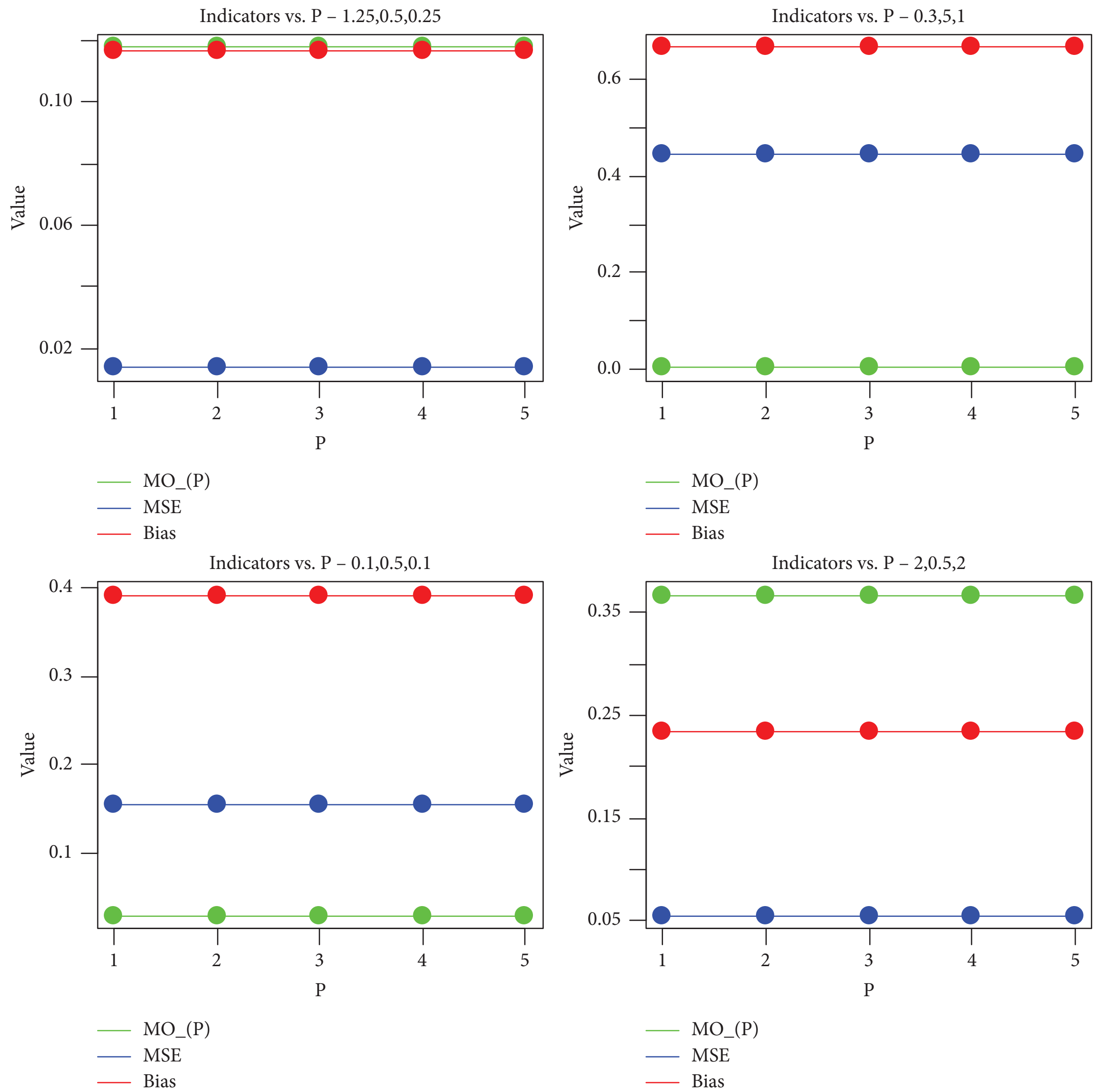

Figure 12: $\mathrm{MOP}_{(P)}$, MSEs, and biases v P.

Table 6: PORT-VAR analysis for extreme USA indemnity losses.

CLs (%)	Number of PORTs	Min.; Max.	1^{st} Qu.; 3^{rd} Qu.	Median; ExV
70	300	48,349; 2,173,595	65,000; 172,000	100,000; 158,009
75	748	12,100; 2,173,595	20,000; 75,000	35,000; 77,970
80	1017	5003; 2,173,595	11,280; 55,000	23,000; 59,573
85	1347	1522; 2,173,595	5450; 40,750	15,000; 45,791
95	1395	1075; 2,173,595	5000; 40,000	14,875; 44,263
99	1484	165.0; 2,173,595	4028; 35,000	12,500; 41,652

management strategies within the insurance sector. These data are crucial for understanding how extreme events may impact indemnity claims and emphasizes the necessity of robust risk assessment frameworks in insurance practices. Figure 13 complements Table 7 by presenting plots of VAR, T-VAR, TV, and T-MV analyses for extreme USA indemnity losses across CLs. These visual results validate and highlight the findings presented in Table 8. Figure 14 presents the violin plots (left) and densities (right) of PORT-VaR analysis for extreme USA indemnity losses. Figure 15 provides the $\mathrm{MOP}_{(P)}$ $|P=5$, VaR, T-VAR, TV, and TVM analysis for extreme USA indemnity losses. Figure 16 compares the risk indicators for the new and the baseline model.

Based on the analysis of Table 7, the GELO model consistently outperforms the LO model across all risk indicators (VAR, T-VAR, TV, and T-MV) and CLs (70%–

Table 7: $MOP_{(P)}$ assessment under $P = 1, 2, \ldots, 5$ and $n = 5000$.

$P \longrightarrow$	1	2	3	4	5	$MOP_{(P)}$
a_1, a_2, ξ			1.25, 0.5, 0.25			
TMV			0.2,341,351			
MO (P)	0.117,788	0.117,789	0.1,177,896	0.1,177,902	0.1,177,905	5
MSE	0.01,353,665	0.01,353,641	0.01,353,627	0.01,353,614	0.01,353,605	
Bias	0.1,163,471	0.1,163,461	0.1,163,455	0.1,163,449	0.1,163,445	
a_1, a_2, ξ			0.3, 5, 1			
TMV			0.6,696,952			
MO (P)	0.002,481,716	0.002,710,072	0.003,027,622	0.003,444,808	0.003,737,608	5
MSE	0.4,451,739	0.4,448,692	0.4,444,457	0.4,438,897	0.4,434,996	
Bias	0.6,672,135	0.6,669,852	0.6,666,676	0.6,662,504	0.6,659,576	
a_1, a_2, ξ			0.1, 0.5, 0.1			
TMV			0.4,210,789			
MO (P)	0.02,880,431	0.02,880,486	0.02,880,519	0.02,880,549	0.02,880,568	5
MSE	0.1,538,794	0.1,538,789	0.1,538,787	0.1,538,785	0.1,538,783	
Bias	0.3,922,746	0.3,922,741	0.3,922,737	0.3,922,734	0.3,922,732	
a_1, a_2, ξ			2, 0.5, 2			
TMV			0.6,003,825			
MO (P)	0.3,672,511	0.367,255	0.3,672,574	0.3,672,595	0.3,672,608	5
MSE	0.05,435,027	0.05,434,843	0.05,434,735	0.05,434,637	0.05,434,573	
Bias	0.2,331,314	0.2,331,275	0.2,331,252	0.2,331,231	0.2,331,217	

Table 8: VAR, T-VAR, TV, and T-MV analysis for extreme USA indemnity losses.

q ↓risk indicator $\longrightarrow$ (%)	$MOP_{(P)}$	VAR	T-VAR	TV	T-MV
GELO model					
70	0.03,280,087	0.1,184,583	0.06,598,845	0.0007,966,466	0.005,149,352
80	0.03,280,087	0.07,982,866	0.05,004,398	0.0003,696,716	0.002,872,839
90	0.03,280,087	0.04,972,803	0.03,416,273	0.0001,353,883	0.00130,159
95	0.03,280,087	0.03,510,078	0.02,395,399	$4.069509e-05$	0.0006,139,461
99	0.03,280,087	0.01,785,266	0.0147,791	$1.235666e-05$	0.0002,299,546
LO model					
70	0.9,910,138	0.9,987,070	0.9,949,748	0.0001,690,705	0.9,901,436
80	0.9,910,138	0.9,979,075	0.9,928,553	0.0002,606,078	0.9,860,215
90	0.9,910,138	0.9,964,049	0.9,884,941	0.0004,734,601	0.9,775,910
95	0.9,910,138	0.9,949,285	0.9,850,218	0.0006,531,135	0.9,709,147
99	0.9,910,138	0.9,743,748	0.9,443,125	0.0023,713,240	0.8,939,492

99%). Therefore, if the criterion is that lower values indicate better performance in managing extreme indemnity losses, insurance companies should prefer the GELO model for its superior risk management capabilities as indicated by the lower values in VAR, T-VAR, TV, and T-MV metrics. This choice ensures better preparation and resilience against extreme events that could impact indemnity losses.

In other words,

1. Across all risk indicators (VAR, T-VAR, TV, and T-MV), the GELO model consistently exhibits lower values compared to the LO model. Lower values in these metrics indicate that the GELO model predicts and manages extreme indemnity losses more effectively.
2. The GELO model's ability to maintain lower VAR values suggests a stronger capability to limit potential losses within specified confidence intervals. This is crucial for insurers as it indicates a proactive approach in safeguarding against unexpected financial liabilities arising from extreme events.
3. In terms of T-VAR, TV, and T-MV metrics, which focus on tail risk management and extreme loss scenarios, the GELO model again demonstrates superiority. Lower T-VAR values signify better preparation for rare but severe events, ensuring that the insurer is adequately prepared for worst-case scenarios.
4. Opting for the GELO model enhances an insurance company's resilience against catastrophic events. By consistently achieving lower values in these risk indicators, insurers can better withstand financial shocks and maintain stability even in turbulent market conditions.
5. Given the competitive and volatile nature of the insurance industry, choosing the GELO model aligns with strategic risk management objectives. It reflects a commitment to robust risk assessment practices that

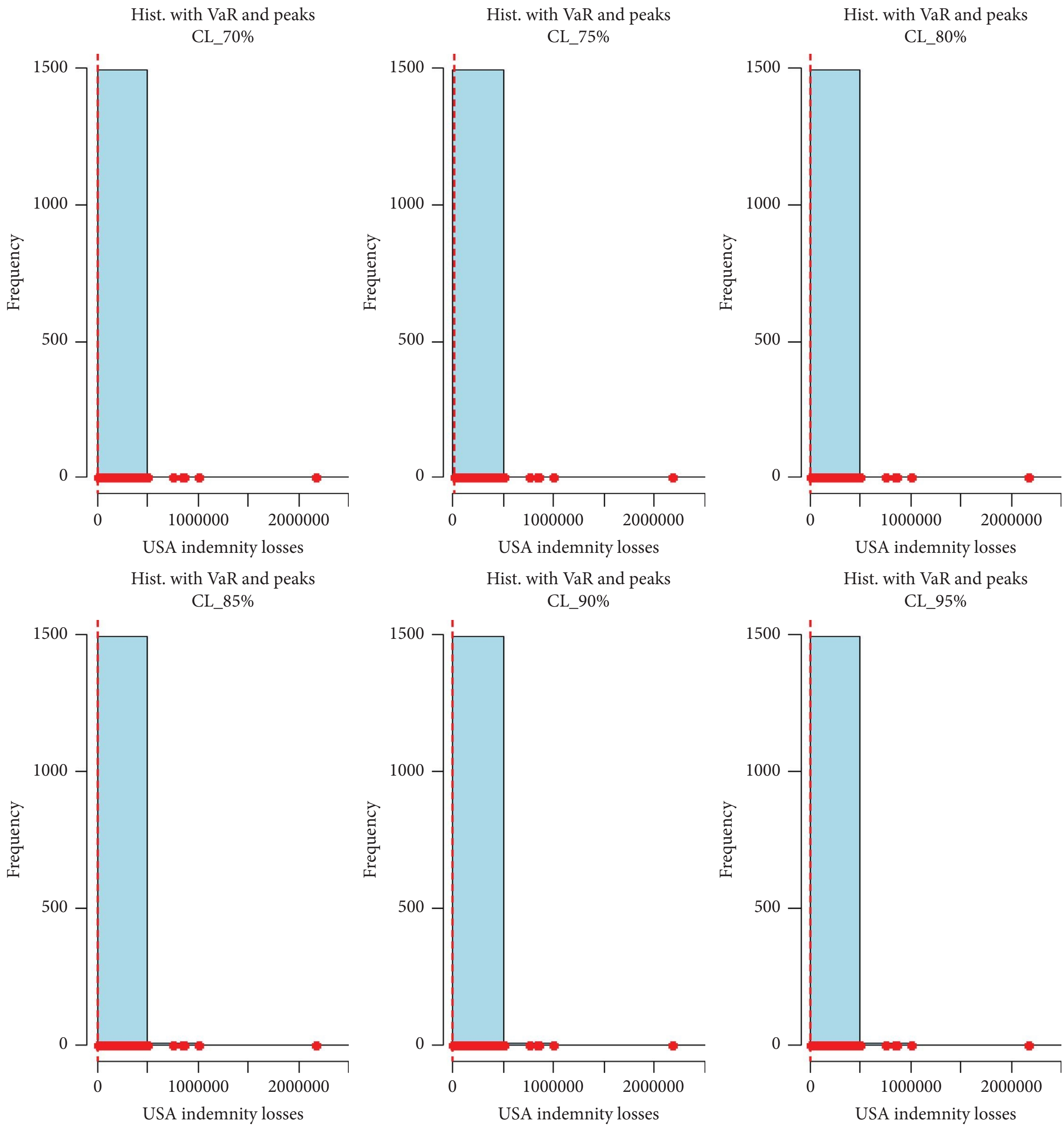

Figure 13: PORT-VaR analysis for extreme USA indemnity losses.

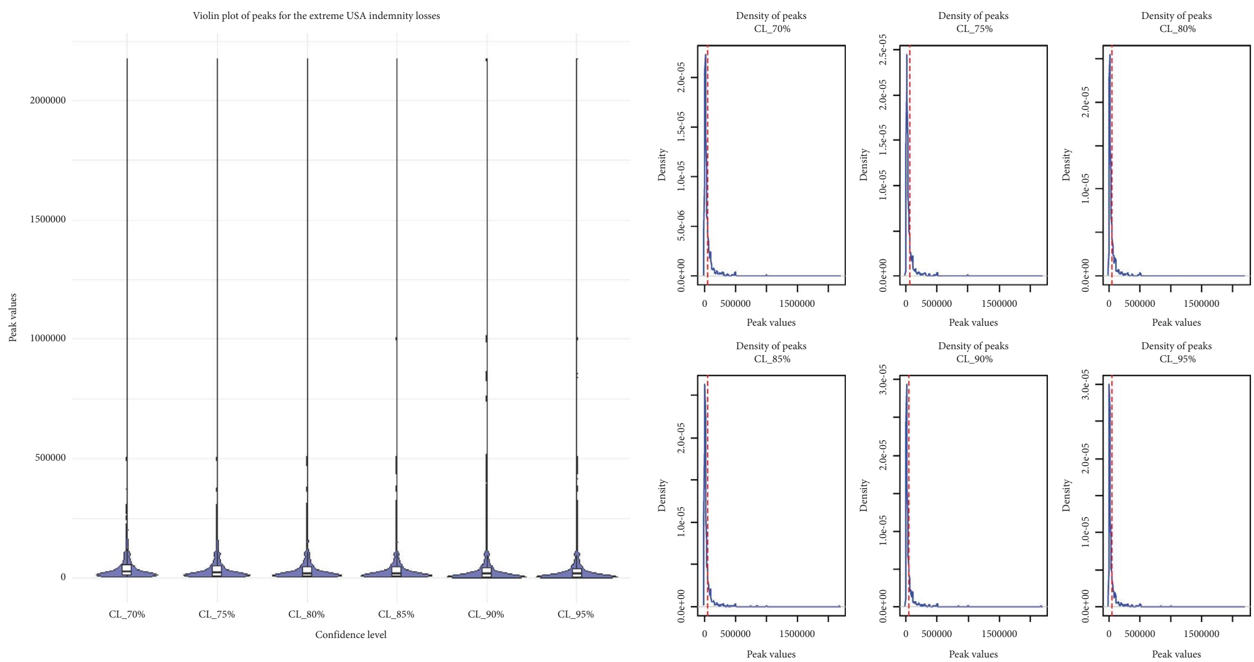

(a) (b)

Figure 14: Violin plot (a) densities (b) of PORT-VaR analysis for extreme USA indemnity losses.

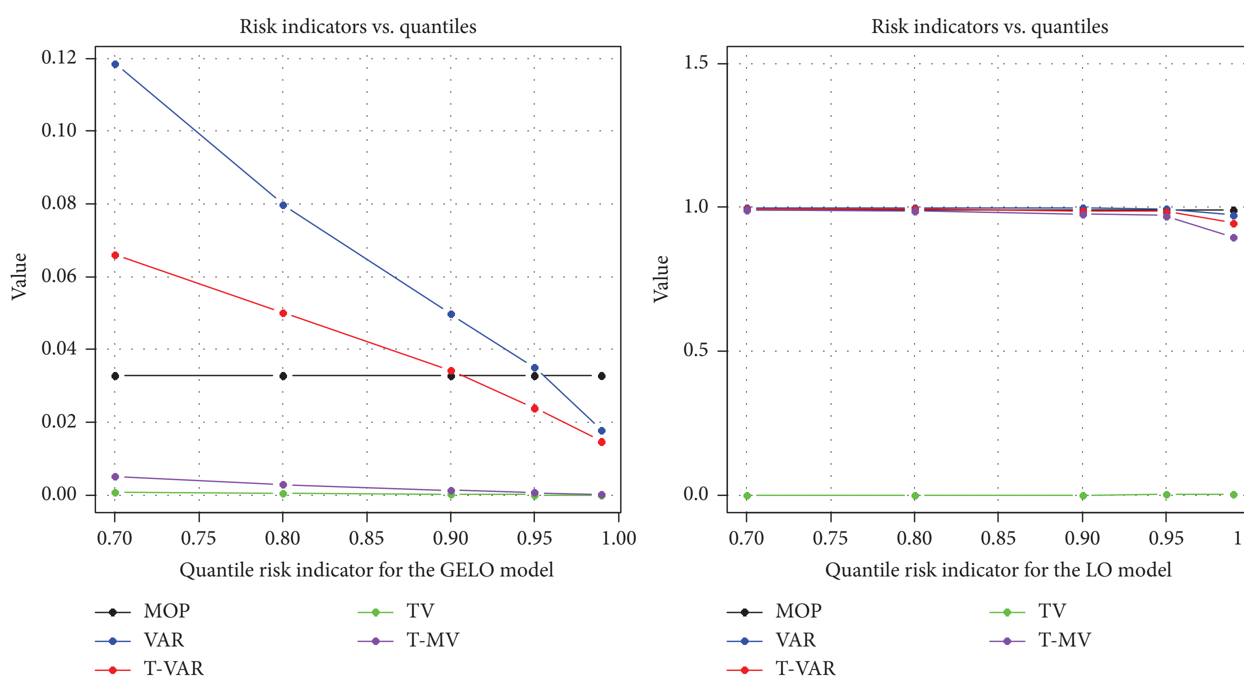

Figure 15: $\mathrm{MOP}_{(P)}|p=5$, VaR, T-VaR, TV, and TVM analysis for extreme USA indemnity losses v the CLs.

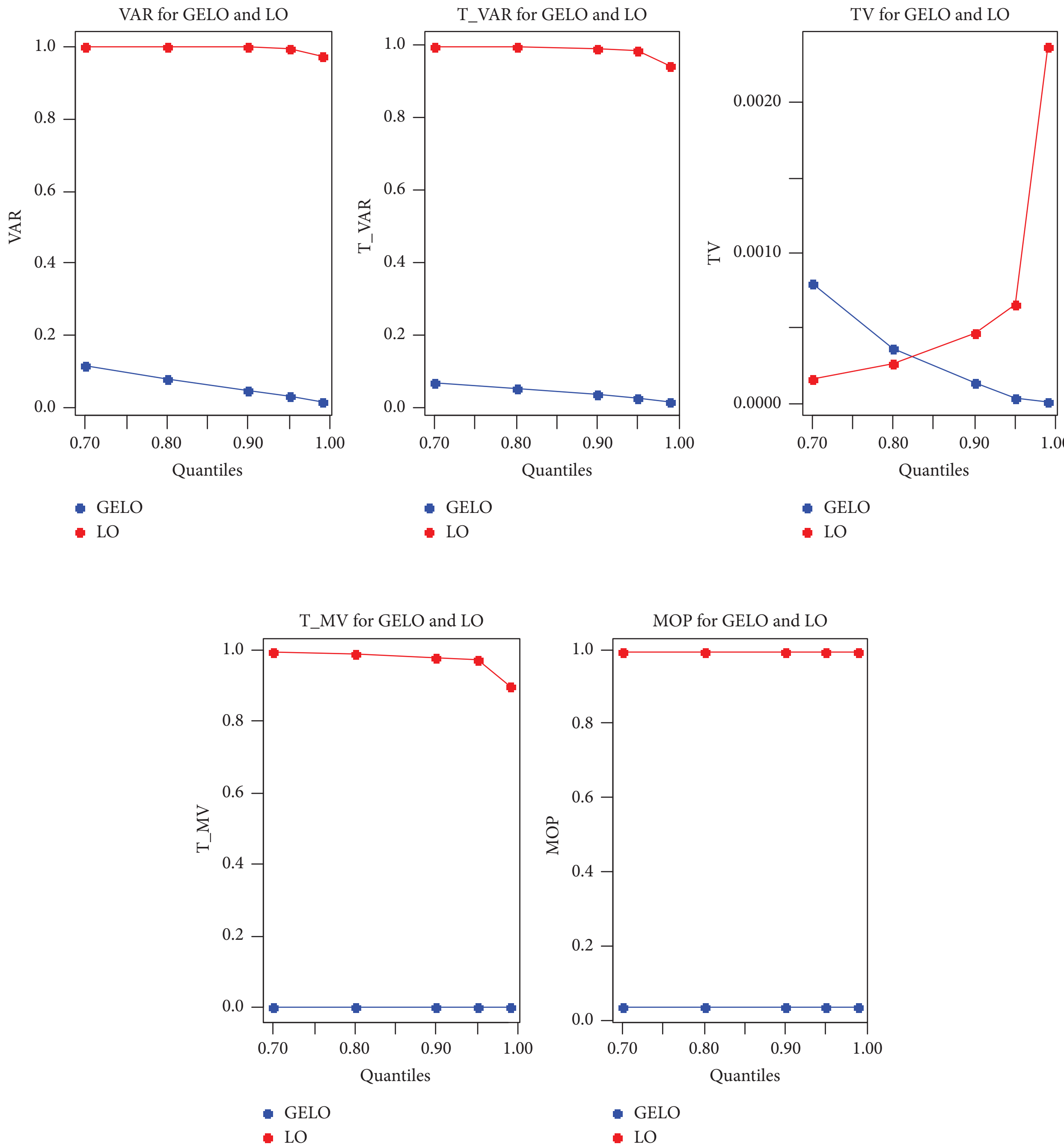

Figure 16: Comparing the risk indicators for the new and the baseline model.

not only comply with regulatory requirements but also enhance overall operational efficiency and profitability.

6. The preference for the GELO model underscores its potential to contribute to long-term sustainability. By minimizing potential losses at various CLs, insurers can build trust among stakeholders and maintain a strong market position amid uncertainties.

8. Conclusions

This study focuses on investigating a new generalized LO lifetime model. The new density function can emerge in four ways: "asymmetric and right-skewed PDF," "symmetric PDF," "asymmetric and negative skewed PDF," and "uniformed PDF." The new failure rate function can emerge in many ways such as the "steadily declining failure rate," the "steadily rising failure rate," and the "stable rate of failure." The novel LO density may be shown as a mixture of the exponentiated LO model, and this can be employed in the process of deducing the majority of mathematical findings and derivations. The skewness of the novel LO distribution can be either positive (indicating right skewness) or negative skewness, depending on the value of the skewness parameter. A set of new mathematical descriptions has been created, all of which are based on a unique set of hypotheses. These novel mathematical formulations encompass characterizations derived from TTMs, characterizations derived from the terms of the RvHF, and characterizations derived from the CEx of a specific function of the RV. Furthermore, we shall explore the multivariate generalized odd-generalized exponential LO type. Alternatively, future research could focus on exploring these novel models. The maximum likelihood method is used to obtain a precise estimation of the parameters for the generalized odd-generalized exponential LO distribution. To evaluate maximum likelihood estimators' performance in finite sample circumstances, we ran simulation studies. The terms "biases" and also "MSEs" were employed as our analytical tools. It is worth noting that the Bias for all parameters are generally negative and tend to approach zero as the sample size (n) increases towards infinity. Similarly, the MSEs for all parameters also approach zero as n approaches infinity. The generalized odd-generalized exponential LO model is the most suitable choice among various well-known models. In summary, this paper not only introduces a new heavy-tailed LO model but also delves into its characterizations, copula functions, and mathematical properties. It offers a valuable resource for researchers and practitioners seeking to better understand and model heavy-tailed reliability data. The comprehensive analysis and practical applications discussed in this paper serve to advance the field of reliability analysis and offer a significant contribution to the scientific community. Based on the risk analysis, the following results can be highlighted:

- Across all risk indicators, the new model consistently demonstrates lower values compared to the LO model. These lower values across metrics indicate that the new model effectively predicts and manages extreme indemnity losses. Also, the new model's ability to maintain lower VAR values suggests a heightened capacity to control potential losses within specified confidence intervals. This proactive approach is crucial for insurers as it helps protect against unexpected financial liabilities stemming from severe events.
- Concerning T-VAR, TV, and T-MV metrics, which focus on managing tail risks and extreme loss scenarios, the new model again shows superiority. Lower T-VAR values indicate better readiness for rare but significant events, ensuring insurers are well-prepared for worst-case scenarios. Opting for the new model bolsters an insurance company's resilience against catastrophic events. By consistently achieving lower values in these risk indicators, insurers can withstand financial shocks and maintain stability even in turbulent market conditions.
- Given the competitive and volatile nature of the insurance industry, choosing the new model aligns with strategic risk management goals. It reflects a commitment to robust risk assessment practices that not only comply with regulatory standards but also enhance overall operational efficiency and profitability.
- Preferring the new model underscores its potential to foster long-term sustainability. By minimizing potential losses across various CLs, insurers can instill confidence among stakeholders and sustain a strong market presence amidst uncertainties.

Data Availability Statement

The data used to support the findings of this study are included within the article.

Conflicts of Interest

The authors declare no conflicts of interest.

Funding

The authors received no specific funding for this work.

Acknowledgments

The first author wishes to extent his sincere gratitude to the Deanship of Scientific Research at the Islamic University of Madinah for support provided to the Post-Publication Program (3).

References

[1] K. S. Lomax, "Business Failures: Another Example of the Analysis of Failure Data," *Journal of the American Statistical Association* 49, no. 268 (1954): 847–852, https://doi.org/10.2307/2281544.

[2] P. R. Tadikamalla, "A Look at the Burr and Related Distributions," *International Statistical Review/Revue Internationale de Statistique* 48, no. 3 (1980): 337–344, https://doi.org/10.2307/1402945.

[3] G. M. Cordeiro, E. M. Ortega, and B. V. Popović, "The Gamma-Lomax Distribution," *Journal of Statistical Computation and Simulation* 85, no. 2 (2015): 305–319, https://doi.org/10.1080/00949655.2013.822869.

[4] M. Aboraya, "Marshall-Olkin Lehmann Lomax Distribution: Theory, Statistical Properties, Copulas and Real Data Modeling," *Pakistan Journal of Statistics and Operation Research* (2021): 509–530, https://doi.org/10.18187/pjsor.v17i2.3732.

[5] M. Refaie, "A New Compound Generalization of the Lomax Lifetime Model: Properties, Copulas and Modeling Real Data," *Statistics, Optimization and Information Computing* 10, no. 2 (2022): 484–504, https://doi.org/10.19139/soic-2310-5070-1207.

[6] A. Corbellini, L. Crosato, P. Ganugi, and M. Mazzoli, "Fitting Pareto II Distributions on Firm Size: Statistical Methodology and Economic Puzzles," *Advances in Data Analysis* (2010): 321–328, https://doi.org/10.1007/978-0-8176-4799-5_26.

[7] M. Xie and C. D. Lai, *Statistical Estimation in Extreme Value Distributions With Insurance Applications* (Kluwer Academic Publishers, 1996).

[8] A. V. Asimit and B. L. Jones, "Applications of the Generalized Pareto Distribution in Insurance and Finance," *North American Actuarial Journal* 15, no. 3 (2011): 371–389.

[9] S. A. Klugman, H. H. Panjer, and G. E. Willmot, *Loss Models: From Data to Decisions*, 4th edition (Wiley, 2012).

[10] Q. Tang and X. Wang, "A Class of Pareto-Type Distributions With Applications in Insurance and Finance," *ASTIN Bulletin: The Journal of the International Actuarial Association* 39, no. 1 (2009): 1–21.

[11] A. J. McNeil, R. Frey, and P. Embrechts, *Quantitative Risk Management: Concepts, Techniques and Tools* (Princeton University Press, 2015).

[12] H. S. Mohamed, G. M. Cordeiro, R. Minkah, H. M. Yousof, and M. Ibrahim, "A Size-of-Loss Model for the Negatively Skewed Insurance Claims Data: Applications, Risk Analysis Using Different Methods and Statistical Forecasting," *Journal of Applied Statistics* 51, no. 2 (2024): 348–369, https://doi.org/10.1080/02664763.2022.2125936.

[13] M. Alizadeh, I. Ghosh, H. M. Yousof, M. Rasekhi, and G. G. Hamedani, "The Generalized Odd Generalized Exponential Family of Distributions: Properties, Characterizations and Application," *Journal of Data Science* 15, no. 3 (2021): 443–466, https://doi.org/10.6339/jds.201707_15(3).0005.

[14] M. S. Hamed, G. M. Cordeiro, and H. M. Yousof, "A New Compound Lomax Model: Properties, Copulas, Modeling and Risk Analysis Utilizing the Negatively Skewed Insurance Claims Data," *Pakistan Journal of Statistics and Operation Research* 18, no. 3 (2022): 601–631, https://doi.org/10.18187/pjsor.v18i3.3652.

[15] H. M. Yousof, Y. Tashkandy, W. Emam, M. M. Ali, and M. Ibrahim, "A New Reciprocal Weibull Extension for Modeling Extreme Values With Risk Analysis Under Insurance Data," *Mathematics* 11, no. 4 (2023): 966, https://doi.org/10.3390/math11040966.

[16] H. M. Yousof, S. I. Ansari, Y. Tashkandy, et al., "Risk Analysis and Estimation of a Bimodal Heavy-Tailed Burr XII Model in Insurance Data: Exploring Multiple Methods and Applications," *Mathematics* 11, no. 9 (2023): 2179, https://doi.org/10.3390/math11092179.

[17] M. Ibrahim, W. Emam, Y. Tashkandy, M. M. Ali, and H. M. Yousof, "Bayesian and Non-Bayesian Risk Analysis and Assessment Under Left-Skewed Insurance Data and a Novel Compound Reciprocal Rayleigh Extension," *Mathematics* 2023 (2023).

[18] H. M. Yousof, M. M. Saber, A. H. Al-Nefaie, N. S. Butt, M. Ibrahim, and S. L. Alkhayyat, "A Discrete Claims-Model for the Inflated and Over-Dispersed Automobile Claims Frequencies Data: Applications and Actuarial Risk Analysis," *Pakistan Journal of Statistics and Operation Research* (2024): 261–284, https://doi.org/10.18187/pjsor.v20i2.4535.

[19] I. Elbatal, L. S. Diab, A. B. Ghorbal, H. M. Yousof, M. Elgarhy, and E. I. Ali, "A New Losses (Revenues) Probability Model With Entropy Analysis, Applications and Case Studies for Value-at-Risk Modeling and Mean of Order-P Analysis," *AIMS Mathematics* 9, no. 3 (2024): 7169–7211, https://doi.org/10.3934/math.2024350.

[20] M. Hashempour, M. Alizadeh, and H. M. Yousof, "A New Lindley Extension: Estimation, Risk Assessment and Analysis under Bimodal Right Skewed Precipitation Data," *Annals of Data Science* 11, no. 6 (2023): 1919–1958, https://doi.org/10.1007/s40745-023-00485-1.

[21] M. Alizadeh, M. Afshari, V. Ranjbar, F. Merovci, and H. M. Yousof, "A Novel XGamma Extension: Applications and Actuarial Risk Analysis Under the Reinsurance Data," *São Paulo Journal of Mathematical Sciences* 18 (2023): 407–437, https://doi.org/10.1007/s40863-023-00373-9.

[22] M. Salem, W. Emam, Y. Tashkandy, et al., "A New Lomax Extension: Properties, Risk Analysis, Censored and Complete Goodness-of-Fit Validation Testing Under Left-Skewed Insurance, Reliability and Medical Data," *Symmetry* 15, no. 7 (2023): 1356, https://doi.org/10.3390/sym15071356.

[23] G. G. Hamedani, H. Goual, W. Emam, et al., "A New Right-Skewed One-Parameter Distribution With Mathematical Characterizations, Distributional Validation, and Actuarial Risk Analysis, With Applications," *Symmetry* 15, no. 7 (2023): 1297, https://doi.org/10.3390/sym15071297.

[24] M. Alizadeh, M. Afshari, J. E. Contreras-Reyes, D. Mazarei, and H. M. Yousof, "The Extended Gompertz Model: Applications, Mean of Order P Assessment and Statistical Threshold Risk Analysis Based on Extreme Stresses Data," *IEEE Transactions on Reliability* (2024): 1–13, https://doi.org/10.1109/tr.2024.3425278.

[25] C. Marshall and M. Siegel, "Value-at-Risk: Implementing a Risk Measurement Standard" (1996).

[26] P. Best, *Implementing Value at Risk* (John Wiley and Sons, 2000).

[27] K. Syuhada, V. Tjahjono, and A. Hakim, "Improving Value-at-Risk Forecast Using GA-ARMA-GARCH and AI-KDE Models," *Applied Soft Computing* 148 (2023): 110885, https://doi.org/10.1016/j.asoc.2023.110885.

[28] J. F. Cordero-Romero and S. Benito-Muela, "On the Methodologies of Threshold Selection in the Context of Peaks Over Threshold Approach for Market Risk Modelling" (2023).

[29] S. Benito, C. López-Martín, and M. Á. Navarro, "Assessing the Importance of the Choice Threshold in Quantifying Market Risk Under the POT Approach (EVT)," *Risk Management* 25, no. 1 (2023): 6, https://doi.org/10.1057/s41283-022-00106-w.

[30] M. K. Refaie and E. I. Ali, "A New Reciprocal System of Burr Type X Densities With Applications in Engineering, Reliability, Economy, and Medicine," *Pakistan Journal of Statistics and Operation Research* (2023): 373–394, https://doi.org/10.18187/pjsor.v19i2.4310.

[31] M. K. Refaie, A. A. Yaqoob, M. A. Selim, and E. I. Ali, *A Novel Version of the Exponentiated Weibull Distribution: Copulas, Mathematical Properties and Statistical Modeling* (Pakistan Journal of Statistics and Operation Research, 2023).

[32] J. Martín, M. I. Parra, E. L. Sanjuán, and M. M. Pizarro, "New Bayesian Method for Estimation of Value at Risk and Conditional Value at Risk," *arXiv preprint arXiv:2306.12202* (2023).

[33] W. Glänzel, "A Characterization Theorem Based on Truncated Moments and Its Application to Some Distribution Families," *Mathematical Statistics and Probability Theory (Bad Tatzmannsdorf, 1986)* (1987): 75–84, https://doi.org/10.1007/978-94-009-3965-3_8.

[34] V. Papathanasiou, "Some Characterizations of Distributions Based on Order Statistics," *Statistics and Probability Letters* 9, no. 2 (1990): 145–147, https://doi.org/10.1016/0167-7152(92)90009-t.

[35] W. Glänzel, "Some Consequences of a Characterization Theorem Based on Truncated Moments," *Statistics* 21 (1990): 613–618, https://doi.org/10.1080/02331889008802273.

[36] J. R. M. Hosking, "On the Characterization of Distributions by Their-Moments," *Journal of Statistical Planning and Inference* 136, no. 1 (2006): 193–198, https://doi.org/10.1016/j.jspi.2004.06.004.

[37] M. H. Tahir, G. M. Cordeiro, M. Mansoor, and M. Zubair, "The Weibull-Lomax Distribution: Properties and

Applications," *Hacettepe Journal of Mathematics and Statistics* 44, no. 2 (2015): 455–474.
[38] A. J. Lemonte and G. M. Cordeiro, "An Extended Lomax Distribution," *Statistics* 47, no. 4 (2013): 800–816, https://doi.org/10.1080/02331888.2011.568119.
[39] M. H. Tahir, M. Adnan Hussain, G. M. Cordeiro, G. G. Hamedani, M. Mansoor, and M. Zubair, "The Gumbel-Lomax Distribution: Properties and Applications," *Journal of Statistical Theory and Applications* 15, no. 1 (2016): 61–79, https://doi.org/10.2991/jsta.2016.15.1.6.
[40] M. G. Khalil and E. I. Ali, *A Generalization of Burr Type XII Distribution With Properties, Copula and Modeling Symmetric and Skewed Real Data Sets* (Pakistan Journal of Statistics and Operation Research, 2023).
[41] R. C. Gupta, P. L. Gupta, and R. D. Gupta, "Modeling Failure Time Data by Lehman Alternatives," *Communications in Statistics—Theory and Methods* 27, no. 4 (1998): 887–904, https://doi.org/10.1080/03610929808832134.
[42] D. N. P. Murthy, M. Xie, and R. Jiang, *Weibull Models* (Wiley, 2004).
[43] A. Aljadani, "Assessing Financial Risk With Extreme Value Theory: US Financial Indemnity Loss Data Analysis," *Alexandria Engineering Journal* 105 (2024): 496–507, https://doi.org/10.1016/j.aej.2024.08.006.